TCAD Parameters for 4H-SiC: A Review

Jürgen Burin,[1] Philipp Gaggl,[1] Simon Waid,[1] Andreas Gsponer,[1] and Thomas Bergauer[1]

Institute of High Energy Physics, Austrian Academy of Sciences, Nikolsdorfer Gasse 18, 1050 Wien

(*e-mail: juergen.burin@oeaw.ac.at)

(Dated: 21 January 2025)

In this paper we review the models and their parameters to describe the relative permittivity, bandgap, impact ionization, mobility, charge carrier recombination/effective masses and incomplete dopant ionization of 4H silicon carbide in computer simulations. We aim to lower the entrance barrier for newcomers and provide a critical evaluation of the status quo to identify shortcomings and guide future research. The review reveals a rich set of often diverging values in literature based on a variety of calculation and measurement methods. Although research for all the selected parameters is still active, we show that sometimes old values or those determined for other kinds of silicon carbide are commonly used.

Keywords: 4H-SiC, TCAD simulations, simulation parameters, silicon carbide

CONTENTS

E_g	band gap energy	T	temperature
$\hbar$	reduced Plank constant	m_d^*	effective density-of-state mass
ε	permittivity	e	elementary charge
m_0	electron rest mass	ε_0	vacuum permittivity
E_F	intrinsic Fermi energy	t	time
E_C	conduction band energy	E_V	valence band energy
n_i	intrinsic carrier concentration	F	electric field
N_A	acceptor concentration	N_D	donor concentration

I. INTRODUCTION

Silicon carbide (SiC) is a wide band gap semiconductor that is increasingly deployed in harsh or high voltage applications due to its favorable properties of high breakdown voltage, low leakage current or fast switching speed[1]. The respective devices are designed using *technology computer aided design* (TCAD) simulations that are able to decrease the amount of required design iterations by predicting the final behavior. To achieve accurate results, a wide range of physical properties are described by more or less complex models, which all rely on a certain set of parameters. The have to be provided by the user, whereat reliable results can only be achieved if the chosen parameter set is suitable.

For 4H-SiC, the most prominent polytype of silicon carbide, the main issue with TCAD simulations is not the lack of parameters in literature but rather the overwhelming amount. Over a time span of more than a century numerous investigations proposed models and parameters for a wide range of physical parameters, resulting in two essential problems: 1) For newcomers a proper selection of parameters is challenging due to the available data. The sometimes contradicting literature also demands some time before a topic can be fully understood. 2) A lot of effort is required to trace values back to their origin. This step is, however, crucial to identify shortcomings in the status quo and trigger a critical (re-)evaluation of single properties. Overviews that compare a subset of the available models with often solely one set of parameters have been published for the topics impact ionization[2–4], band gap[5,6], charge carrier recombination[7] and mobility[6]. All these publications lack, however, a proper discussion of the origin of the presented values, possible shortcoming and suitable avenues for future research.

In this paper we, thus, conduct a literature review on TCAD parameters for 4H-SiC focused on

the topics relative permittivity, density-of-states mass, band gap, impact ionization, charge carrier recombination, incomplete ionization and mobility. For each we describe the theoretical models and provide a simple overview of the topic to decrease the entrance barrier for newcomers. We also present the achieved parameters, analyze the agreement within the scientific community and comment on the suitability of the most commonly used parameters. We further identify possible shortcomings to guide future research. Nevertheless, we want to highlight that our results are not a one fits all solution but mainly an overview for starting parameter sets, that have to be further refined to fit the measurements of device at hand.

This paper is organized in the following fashion: In **??** we introduce the general methods utilized in the review followed by an introduction to (4H) silicon carbide in **??**. We then review the models and parameters for the topics permittivity (**??**), density-of-states mass (**??**), band gap (**??**, impact ionization (**??**), charge carrier recombination (**??**), incomplete ionization (**??**) and mobility (Section II). We finally conclude our paper in **??**.

II. MOBILITY

To describe the conductivity ρ of a material[8], which is relevant for any transient process, the charge carrier mobility μ as shown in Eq. (1)[9,10] is used. In this case, n denotes the amount of charge carriers and μ_n the respective mobility. Different mechanisms may influence the mobility such as the surface, the inversion channel in MOS structures and the bulk[8], whereat we will investigate here solely the latter. We, thereby, build on the analysis of measurements by Darmody and Goldsman[11] and the summaries of mobility models published by Neila Inglesias[12], Stefanakis and Zekentes[5] and Tian *et al.*[6].

$$\rho = \frac{1}{nq\mu_\mathrm{n}} \tag{1}$$

Overall, our analyses reveal many investigations targeted toward the mobility.

A. Theory

Charge carriers in 4H-SiC accelerate along the electric field F until they are "scattered", i.e., they drastically change their velocity and/or direction by interacting with other particles. It is possible to distinguish (i) phonon (ii) defect and (iii) carrier-carrier scattering, which can be further divided[13]. The most prominent processes for 4H-SiC are acoustic phonon, (non-)polar optical

phonon, zero and first order optical intervalley phonon, ionized/neutral impurity and carrier-carrier scattering[14–18]. The mobility defines the average time between two scattering event[19] and thus provides a link between charge carriers and scattering processes[20]. Detailed theoretical analyses of each single contribution is available in literature[12,13,15,17,21–24].

In TCAD tools, however, such detailed models are not convenient[17]. Instead, empirical models are used to describe the mobility in the low-field and high-field region (a detailed explanation follows in the next sections). The mobility, thereby, depends on many factors such as doping concentration[25], degree of compensation[26], spatial direction[27–29], temperature[25] and whether majority or minority charge carriers[13] are described. For holes even the separate valence bands (heavy-hole, light-hole, split-off; see **??**)[13,15,30] have to be considered.

In the past years hopping conduction, also denoted as nearest-neighbor-hopping (NNH)[31] or variable-range-hopping (VRH)[31] was described in 4H-SiC. This process describes the tunneling of charge carriers bound to a dopant from one impurity to the next, possible alternated by some conventional drifting phases in the bands. This effect was described at temperatures below 100 K[32] ant at very high doping concentrations[31,33]. Darmody and Goldsman [11] calculated the critical limit for the latter to $N_{\text{crit}} \approx 1 \times 10^{20}/\text{cm}^3$. Since this is a relatively new effect the available information are very limited and we will, thus, not further consider it in this review.

1. Low-Field Mobility

For low electric fields exists a direct relationship between the carrier velocity v and the electric field strength F[34] as shown in Eq. (2). The impact of phonon and impurity scattering is thereby not independent[35], meaning that both have to be implemented in the same model.

$$v = \mu(N,T)F \tag{2}$$

Each dopant represents a coulomb scattering center[10] that causes the charge carrier mobility to decrease. To account for this fact an empirical model shown in Eq. (3) was developed by Caughey and Thomas[36]. μ_{min} can be interpreted as the mobility for very high doping where impurity scattering is dominant[5,12] and μ_{max} the highest possible mobility at low doping, i.e., when lattice (phonon) scattering is dominant[5,8,12]. N_{ref} denotes the doping concentration where the mobility is exactly in between those values[26,34] and δ just how quickly the change from one to the other occurs. Arora, Hauser, and Roulston[37] later simplified the model by replacing the expression

$\mu_{max} - \mu_{min}$ by μ_0[38], which will become interesting when we later investigate the temperature dependency.

$$\mu(N) = \mu_{min} + \frac{\mu_{max} - \mu_{min}}{1 + (N/N_{ref})^{\delta}} \tag{3}$$

There is some disagreement in literature (discussed by Vasilevskiy *et al.* [39]) whether N denotes all dopants[5,16,17,38–58] or just the ionized ones[14,54,59–64]. An argument to use all dopants was that this model is just a fitting[5,6] or that also scattering on neutral dopants decreases the mobility. Roschke and Schwierz [34] stated that using something different than the absolute doping for N did not result in better results but led to convergence issues.

A similar dependency can be observed with changing temperatures. In hot samples more phonons are generated, which increases the probability of a charge carrier's scattering[10,25,65]. In contrast, at low temperatures and high doping concentration (un)ionized impurity scattering is dominant[66]. This is accounted for by scaling the respective parameters with temperature as shown in Eq. (4)[49,67]. Note that $\gamma_{NNref} = -\delta\gamma_{ref}$.

$$\theta = \theta_{300}\left(\frac{T}{300}\right)^{\zeta} \tag{4}$$

$$\theta \in [\mu_{min}, \mu_{max}, \mu_0, N_{ref}, \delta, (N/N_{ref})^{\delta}] \tag{5}$$

$$\zeta \in [\gamma_{min}, \gamma_{max}, \gamma_0, \gamma_{ref}, \gamma_{\delta}, \gamma_{NNref}] \tag{6}$$

We want to highlight that many different names for this combined model exist in literature, featuring sometimes more and sometimes less of the shown temperature scaling factors. Referenced were, among others, the publications by Mohammad *et al.* [68] and Sotoodeh, Khalid, and Rezazadeh [69]. The term Masetti model[25,61] is also used for this model, although the expression proposed by Masetti, Severi, and Solmi [70] actually contains an additional additive term that leads to a further reduction of the mobility at high doping densities (see)[71]. Except for Zhang and You [72] the parameters are, however, chosen in a fashion that the description in Eq. (3) is achieved[8,73].

$$\mu(N) = \mu_{min} + \frac{\mu_{max} - \mu_{min2}}{1 + (N/N_{ref})^{\delta}} - \frac{\mu_1}{1 + (N_{ref2}/N)^{\kappa}} \tag{7}$$

In this model each parameter has a constant temperature scaling parameter. However, depending on the dominant scattering process vastly deviating temperature dependencies have been observed[55]. While acoustic phonon scattering shows a decrease proportional to $T^{-1.5}$[19,40,74–76] the decline proportional to $T^{-2.6}$ was attributed to nonpolar optical phonon scattering[17,76] ($T^{-2.5}$ for optical-mode phonons[19]) . For the latter Adachi [13] states, however, a dependency according

to $T^{-1.5}$. Ionized impurities scale with $T^{3/2}$[16,50,74,75] and neutral impurities with T^{0}[13,16,50] while coulomb scattering scales with T^{1} and phonon scattering with T^{-1}[77]. This makes the model presented in Eq. (3) not adequate for large temperature swings[78]. A different approach was shown by Schröder[35], p. 668 who defined equations below/above 200 K with deviating temperature scaling, but only provided parameters for Si.

To account for the changing temperature behavior Izzo *et al.*[79] used the phenomenological function shown in Eq. (8), without however specifying the values of A and B. This description features an increasing mobility due to ionized impurity scattering at low temperature ($T^{3/2}$) and a adjustable decrease for high temperatures, e.g., $n = 3.06$ in this case. This corresponds to the values by La Via *et al.*[80].

$$\mu(T) = \left(\frac{A}{T^{3/2}} + \frac{B}{T^{-n}} \right)^{-1} \tag{8}$$

Rambach *et al.*[74,75] stated that the parameters of Eq. (3) should be dependent on the doping concentration, without, however, explicitly stating a mathematical expression for these. Rambach, Bauer, and Ryssel[75] also proposes a single temperature scaling for all parameters. Another possibility is to use only a single multiplicative factor for the temperature scaling, that is, however, structured according to the CT equation itself as shown in Eq. 9 and Eq. 10[81,82].

$$\mu_{\mathrm{p}}(T, N_{\mathrm{A}}) = \mu_{\mathrm{p}}(300, N_{\mathrm{A}}) \left(\frac{T}{300} \right)^{\beta_{\mathrm{p}}(N_{\mathrm{A}})} \tag{9}$$

$$\beta_{\mathrm{p}}(N_{\mathrm{A}}) = \beta_{\mathrm{min}} + \frac{\beta_{\mathrm{max}} - \beta_{\mathrm{min}}}{1 + (N_{\mathrm{A}}/N_{\mathrm{p}})^{\eta}} \tag{10}$$

Uhnevionak[83] split μ_{max} into two additive parts with separate temperature scaling as shown in Eq. (11) to simulate the temperature dependent contribution of the bulk mobility on the channel mobility of a MOSFET. The author differentiates between this contribution and the mobility solely in bulk material.

$$\mu_{\mathrm{max}} \left(\frac{T}{300} \right)^{\gamma_{\mathrm{max}}} = \mu_{\mathrm{max1}} \left(\frac{T}{300} \right)^{\gamma_{\mathrm{max1}}} + \mu_{\mathrm{max2}} \left(\frac{T}{300} \right)^{\gamma_{\mathrm{max2}}} \tag{11}$$

Based on Eq. (3) Mnatsakanov *et al.*[66] separated the empirical description in the lattice and charge impurity scattering and scaled these independently with temperature. This leads to the expressions shown in Eq. 12 and Eq. 13 with γ_{I} the temperature scaling factor of the impurity scattering contribution. For $T = T_0$ this expression collapses to Eq. (3). Mnatsakanov *et al.*[66] claims that this model describes the temperature behavior for low and high doping in an improved

fashion. In our opinion the exponents $\gamma_1 + \gamma_{\max}$ and γ_1 should be exchanged such that the nominator is scaled with $(T/T_0)^{\gamma_1+\gamma_{\max}}$ and the denominator with $(T/T_0)^{\gamma_1}$. Also, δ in the nominator of $B(N)$ should be negative. We confirmed this by comparing the results to the figures by Neimontas *et al.* [84] and an analytic comparison to the equation presented by Mnatsakanov, Pomortseva, and Yurkov [85].

$$\mu(N,T) = \mu_{\max}(T_0)\frac{B(N)\left(\frac{T}{T_0}\right)^{\gamma_1}}{1+B(N)\left(\frac{T}{T_0}\right)^{\gamma_1+\gamma_{\max}}} \tag{12}$$

$$B(N) = \left[\frac{\mu_{\min}+\mu_{\max}\left(\frac{N_{\text{ref}}}{N}\right)^{\delta}}{\mu_{\max}-\mu_{\min}}\right]\Bigg|_{T=T_0} \tag{13}$$

One final model was proposed by Klaassen [86] as a unified description of majority and minority charge carriers including screening effects, also called Philips model, which was recently used in conjunction with 4H-SiC[78]. Although this model is already included in state of the art simulation frameworks we did not consider it in our review as no explicit parameters for 4H-SiC were found in literature.

2. *High-Field Mobility*

At high electric fields the charge carrier velocity approaches a maximum value, the so-called saturation velocity. Explanations for this behavior are an increasing amount of optical phonon scattering[25,47,87] or an increase in elastic and nonelastic scattering owing to the increase in carrier energy[49]. Because the velocity is modeled according to $v = \mu F$, the mobility has to decrease. This field dependency of the mobility was, again, modeled by Caughey and Thomas [36] as shown in Eq. (14). Chen *et al.* [88] used the hydrodynamic version instead.

$$\mu = \frac{\mu_{\text{low}}}{\left[1+\left(\frac{\mu_{\text{low}}F}{v_{\text{sat}}}\right)^{\beta}\right]^{\frac{1}{\beta}}} \tag{14}$$

Here μ_{low} denotes the low field mobility as described in the previous section and v_{sat} the saturation mobility (Kimoto and Cooper [89] calls the latter sound velocity). In some cases an additional additive factor α is introduced in various spots of this equation[52,90] but is always set to 0 and, thus, irrelevant.

Because v_{sat} is temperature dependent[10,13,91] Canali *et al.* [92] suggested to scale the parameters β and v_{sat} with temperature, as shown for the low-field case in Eq. (4)[19,49]. This model is thus often called Canali model[93,94]. In some occasions[67] the temperature change of v_{sat} is modeled by the approach presented for Si shown in Eq. (15)[95,96]. Be aware that some publication[12,14,34] use a value of $d = 0.6$, while others use $d = 0.8$ in the denominator, referencing an early edition of Sze and Ng[97].

$$v_{\text{sat}} = \frac{v_{\text{max}}}{1 + d \exp\left(\frac{T}{600}\right)} \,. \tag{15}$$

Also for the temperature scaling of β a slightly different approach shown in Eq. (16) was proposed which is a combination of the modeling by Roschke and Schwierz[34] and Bertilsson, Harris, and Nilsson[98].

$$\beta = \beta_0 + a \exp\left(\frac{T - T_{\text{ref}}}{b}\right) + c\,T \tag{16}$$

Recent Monte-Carlo simulations[12,14,42,98–106] revealed a velocity overshoot, i.e., negative differential mobility, at fields near $1 \times 10^6\,\text{V/cm}$[34]. Foutz, O'Leary, and Shur[107] proposed a new model for wide band gap materials that better models mobility overshoot as shown in Eq. (17)[14]. This approach was used for GaN[108] and lately also for 4H-SiC[14] but is not yet available in TCAD tools. A simplified version ($\alpha = -\infty$) is denoted as transferred-electron model[23,109].

$$v(F) = \frac{\mu_0 F + \mu_1 F (F/F_0)^{\alpha} + v_{\text{sat}} (F/F_1)^{\beta}}{1 + (F/F_0)^{\alpha} + (F/F_1)^{\beta}} \tag{17}$$

We want to highlight that in any of the publications that presented these decreasing velocity the term "overshoot" was stated. In addition the peak value, i.e., the maximum, was denoted as the saturation velocity, which begs the question whether the decrease in velocity is not only a simulation artifact.

Baliga[10] used the presentation shown in Eq. (18) to describe the high field mobility. The parameters from Eq. (3) can be achieved by using $v_{\text{sat}} = A$ and $\mu_{\text{low}} = v_{\text{sat}}/B^{1/\beta}$.

$$\mu = \frac{A}{[B + F^{\beta}]^{1/\beta}} \tag{18}$$

3. Carrier-Carrier Scattering

This scattering process decreases the mobility at high injections levels[6,10,110] and denotes interactions among the same type of charge carriers, e.g., electron-electron[13], or between electrons and holes[26]. To describe this effect the Conwell-Weisskopf equation shown in Eq. (19) is used[44,111–113].

$$\mu_{\mathrm{ccs}} = \frac{D\left(\frac{T}{T_0}\right)^{\frac{3}{2}}}{\sqrt{np}}\left[\ln\left(1+F\left(\frac{T}{T_0}\right)^{2}(pn)^{-\frac{1}{3}}\right)\right]^{-1} \tag{19}$$

4. *Hall Scattering Factor*

The mobility can be experimentally extracted from conductivity measurements, called in that case conductivity or drift mobility, as shown in Eq. (1)[13]. Since the amount of charge carriers is required as well often Hall measurements are used to determine the mobility. In general it is said that the Hall mobility can be easier measured, while the conductivity mobility can be easier calculated[13]. However, for Hall measurements a slightly different mobility, the Hall mobility μ_{H} is determined[114]. The relation between these two is called Hall factor r and defined as shown in Eq. (20)[13,16,28,40,65,115]. In Hall measurements the Hall coefficient R_{H} is determined, that is defined as shown in Eq.(21) with n_{H} the Hall charge carrier count[17,54,116–118]. R_{H} is also used to connect the conductivity and the mobility as shown in Eq. (22)[10,119,120]. For holes the calculation of r_{H} requires to consider both light and heavy holes[15,121].

$$r_{\mathrm{H}} = \frac{\mu_{\mathrm{H}}}{\mu_{\mathrm{c}}} = \frac{n}{n_{\mathrm{H}}} \tag{20}$$

$$R_{\mathrm{H}} = \frac{1}{n_{\mathrm{H}}e} = \frac{r_{\mathrm{H}}}{ne} \tag{21}$$

$$\mu_{\mathrm{H}} = \sigma R_{\mathrm{H}} = \frac{1}{en_{\mathrm{H}}\rho} \tag{22}$$

$$\tag{23}$$

For this reason a clear distinction between Hall and conductivity mobility is shown in the sequel. For further theoretical analyses and overviews on Hall mobilities and measurements the interested reader is referred to the dedicated literature[12,22,122,123].

B. Results & Discussion

In the following we present the gathered results. We had to exclude publications that solely focused on channel mobilities[38,93,124–130], that did not clearly specify the SiC polytype[35,131–134] or that deal with mobility over irradiation defects[135]. Furthermore, we did not consider Wright [136] that got superseded by Wright *et al.* [137].

1. *Measurements*

Several approaches to determine the mobility have been proposed in the literature. These include simulations such as Monte Carlo[42,100,103–106,138,139], full band monte carlo (FBMC)[140], empirical pseudo potentials (EPM)[101,102,104], monte carlo particle (MCP)[30], non equilibrium statistical ensemble formalism (NESEF)[141], linear augmented plane wave (LAPW)[142], density functional theory (DFT)[54], extraction from the diffusion coefficient (DIFF)[84], conductivity tensor calculations (COTE)[27,28,143,144], general calculations[15,21,22] and fitting (FIT)[14,19,20,32,34,49,81,85,93]. Measurements include collected charge (CCh)[145], nanosecond pulsed conductance (NPC)[128,146–149], resistance measurements (RES)[79,80], Schottky barrier diode I-V fitting (SBD-IV)[150], Raman scattering (Raman)[29,151], low temperature photoluminescence (LTPL)[50], spectroscopic ellipsometry (SE)[152], optical detection of cyclotron resonance (ODCR)[24,153], diode I-V (DIV)[150,154], bipolar transistor I-V (BIV)[4] and Hall measurements[16,17,39,40,57,58,60,62,65,74,76,82,114,117,120,155–174]. Regarding the type of mobility the majority of publications provided Hall mobility data[15–17,21,22,27,39,40,57,58,60,62,
and only few directly the conductivity one[24,29,42,140,151].

As outlined in the previous section, the results of the latter have to be scaled by the Hall scattering factor r_H to achieve the conductivity mobility. In early investigations r_H was assumed approximately unity[11,19,34,125,163] due to a lack of reliable data[65]. Later it was shown, however, that this is actually only the case for high magnetic fields[122]. More thorough investigations revealed a dependency on the magnetic field[118,122,175], temperature[15,17,28,54,115,120–122,168,169,176] and doping concentration[54,116,176]. r_H thereby shows predominantly variations in the range of $[0.5, 1.5]$.

Both an increase[58] and a decrease[28,116] of r_H with increasing temperature was observed in measurements, which may even depend on the doping concentration[58]. Pernot, Contreras, and Camassel[15] provided a fitting of the results by Pensl *et al.*[115] as shown in Eq. (24). Theoretical analyses predicted an increase of r_H[17,28].

$$r_\mathrm{H} = 1.748\,23 - 6.22\times10^{-3}T + 1.367\,29\times10^{-5}T^2 - 1.448\,37\times10^{-8}T^3 + 5.864\,98\times10^{-12}T^4 \tag{24}$$

Tanaka *et al.*[54] fitted both the Hall and conductivity mobility with the model shown in Eq. (3). A division of these fittings led to the expression for r_H shown in Eq. (25)

$$r_\mathrm{H} = 1.16\left(\frac{T}{300\,\mathrm{K}}\right)^{-0.9}\frac{1+\left(\frac{T}{300\,\mathrm{K}}\right)^{-1.5}\left(\frac{N_\mathrm{A}}{1\times10^{19}/\mathrm{cm}^3}\right)^{0.7}}{1+\left(\frac{T}{300\,\mathrm{K}}\right)^{-1.8}\left(\frac{N_\mathrm{A}}{3\times10^{18}/\mathrm{cm}^3}\right)^{0.6}} \tag{25}$$

With increasing doping concentration the Hall scattering factor drops[116]. The impact of compensation is still under investigation[17] as well as the anisotropy[118,175].

We want to discuss the publication by Darmody and Goldsman [11] in greater detail here, because it initially seems to provide a simple answer to the question raised above but, in our opinion, contradicts in various occasions the remaining literature. At first the ratio μ_c/μ_H, which is actually the definition of r_H, was defined as the ratio of the free charge carriers and the doping concentration. This is based on the assumption that all dopants contribute to the conductivity mobility, i.e., are ionized, which has to be doubted in 4H-SiC (cp. **??**). The Hall scattering coefficient was set to 1 in this analysis. In the sequel the authors showed two plots, one for the Hall and one for the conductivity mobility, which revealed a significant difference. In detail the latter is much lower, which resulted from the fact that the authors gathered the values from resistivity measurements, assuming that the amount of charge carriers is equal to the doping concentration. Since the presented plots lead to $r_H > 5$ according to the definitions shown in this publication the results of this paper have to be considered with care.

Since there is no simple translation between Hall and conductivity mobility we present the values as published and just denote their meaning with *H* resp. *C* in the sequel.

2. Low-Field Mobility

In literature often only single mobility value is found[268]. Although these can also be used in TCAD tools they often serve the purpose of a rough and quick comparison among different materials. Consequently often no information about doping concentration and temperature are provided. We found a wide range of values for the effective mobility, as well as in single spatial directions (see Fig. 1). The electron mobility is much higher than the hole one, whereat the direction parallel to the c-axis is slightly more beneficial. At least for electrons; for holes no clear distinction is possible. A wide range of values is used in the literature, which reflects the many dependencies of the mobility, e.g., doping concentration, temperature and field strength.

The analysis of the reference chain (see Fig. 2) shows that these values are not derived from a main source but rather smaller clusters are formed. This indicates that the authors assume this as common knowledge, without the need to provide proper references.

As shown before, the mobility shows an anisotropy. Some authors argue that due to low anisotropy (see Table I) just considering mobility in base plane is a reasonable approximation[67],

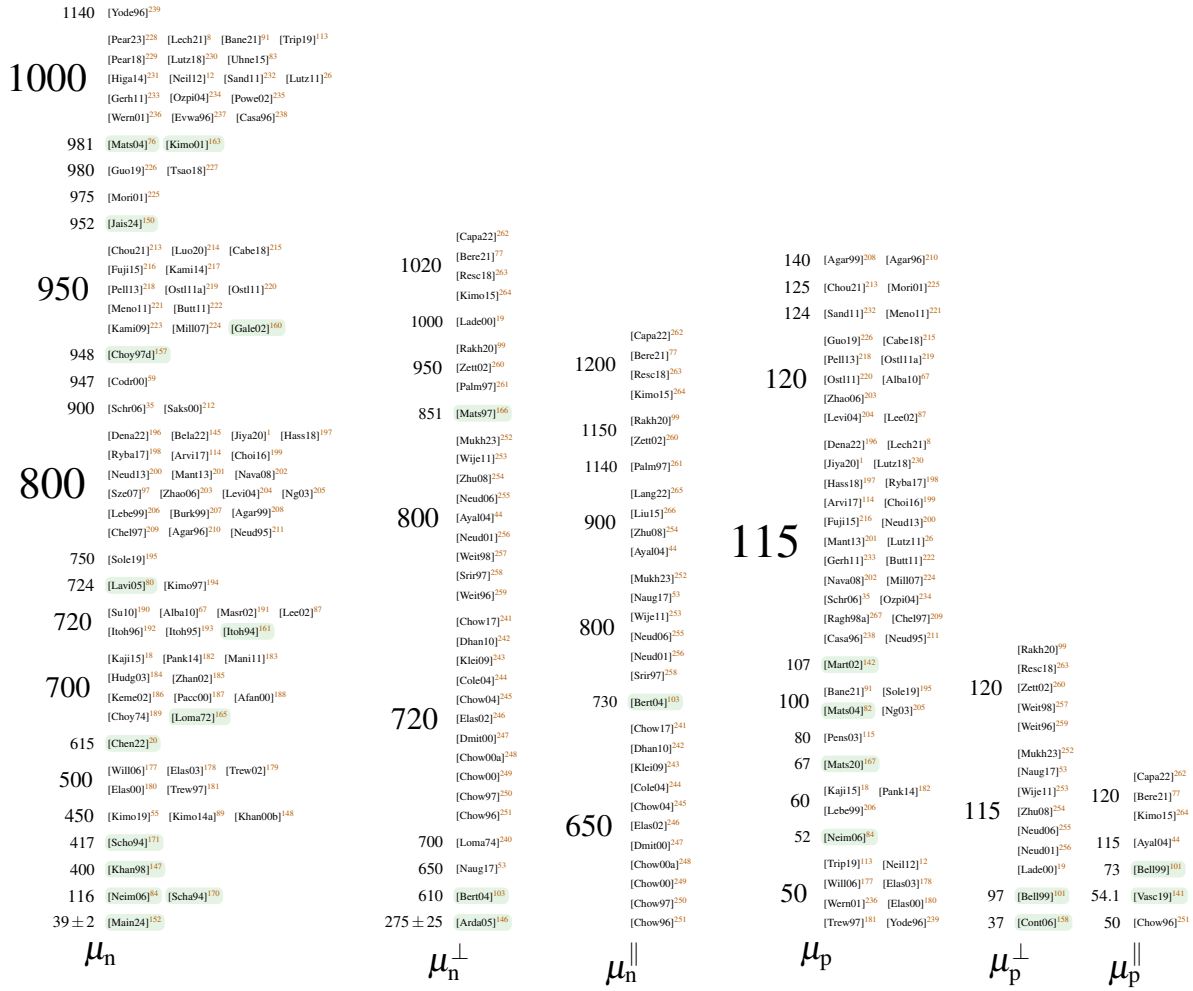

FIG. 1. Single mobility values for 4H-SiC in different spatial directions.

however, Hatakeyama *et al.* [60] showed that not even within the basal plane the mobility is constant. The anisotropy of the mobility is most probably caused by the anisotropy of the effective masses[27,49,57] and thus depends on additional parameters such as the temperature[16]. Although it was pointed out that the ratio changes from below to above one depending on the doping and thus constant values are not well suited[103], almost exclusively constant factors are used in literature (see Fig. 3). Cheng and Vasileska [140] stated that previous publications[40] did not specify the exact perpendicular direction. Thus their values range between 1.25 and 1.75, compared to the previously achieved 1.2[40]. Iwata, Itoh, and Pensl [27] investigated the mobility in varying in-plane directions, revealing a maximum anisotropy factor for electrons of 0.7. The ratio was also investigated over temperature and doping concentration[16,40,42,58,106,120,139,142,170,274]. It was also extracted from ratio of resistivity to cancel the Hall scattering factor[16,57].

FIG. 2. Reference chain for single mobility values in different spatial directions. If only a single value is shown the value denotes the effective value without direction.

For electrons all but one fundamental investigation predict a higher mobility parallel to the c-axis with $\mu_n^\perp/\mu_n^\parallel = 0.83 \pm 0.07$. Some predominantly qualitative overview papers state, however, the opposite[241–247,250,251]. Others predict no anisotropy at all[252,253,255,256,258]. For holes almost all references predict a ratio bigger than one with the most common values of 1.15 ± 0.04.

TABLE I. Fundamental investigations of the ratio of electron and hole mobilities in the direction perpendicular ($\perp$) and parallel ($\parallel$) to the c-axis.

ref.	$\mu_n^\perp/\mu_n^\parallel$ [1]	$\mu_p^\perp/\mu_p^\parallel$ [1]	type[a]	method
[Scha94][170]	0.85 ± 0.05	-	H	Hall
[Scha94][40]	0.83	-	H	Hall
[Hari95][29]	1.2 ± 0.3	-	C	Raman
[Josh95][139]	0.75 ± 0.04	-	C	MC
[Son95][153]	0.7[b]	-	C	ODCR
[Nils96][106]	0.825 ± 0.025	-	C	MC
[Choy97d][157]	0.86	-	H	Hall
[Mats97][166]	$(1.2)^{-1}$	-	H	Hall
[Mick98][42]	0.77 ± 0.07	-	C	MC
[Bell99][101]	-	1.33	C	EPM
[Iwat00][27]	0.7	-	H	COTE
[Bert01][138]	0.85	-	C	MC
[Hata03][60]	0.83	1.15	H	Hall
[Bert04][103]	0.84	-	C	MC
[Chen20][140]	$(1.75)^{-1}$ - $(1.25)^{-1}$	-	C	FBMC
[Ishi21][16]	$(1.15 \pm 0.03)^{-1}$	-	H	Hall
[Ishi24][58]	-	$(0.90 \pm 0.05)^{-1}$	H	Hall

[a] type of mobility: Hall (H), conductivity (C)
[b] temperature range of 2–6 K

a. Doping Dependency A lot of publications investigated the impact of the doping concentration on the low-field mobility[15–17,21,22,24,28,29,39,40,50,54,55,57,58,60,62,76,114,117,122,143,151,156,159,162,166,167,169,17] which makes it impossible to show all gathered results in this paper. Instead we focus on the models that were developed based on these data.

A wide range of parameters for Eq. (3) were proposed to describe the low-field mobility. The model parameters for the electron (see Table II) have been proposed over a range of three decades. The maximum mobility varies within a range of $[800, 1240]$ and the reference doping concentration N_{ref} only minor in the low 10^{17} range. There were several attempts to distinguish the spatial directions and to describe the temperature dependency of the single parameters. We also highlighted

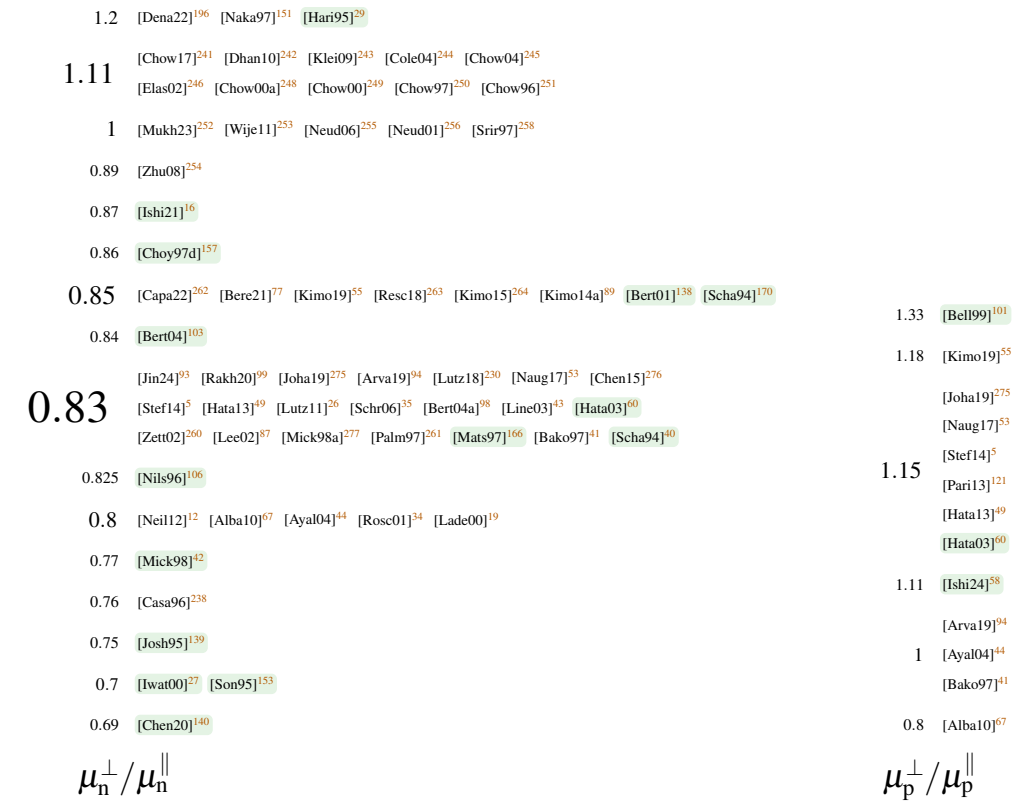

FIG. 3. Ratio of electron and hole mobilities in the direction perpendicular ($\perp$) and parallel ($\parallel$) to the c-axis used in literature.

the deviating interpretation of parameter N in the table, which underlines the large discrepancy in literature.

In a graphical representation (see Fig. 4) the qualitative agreement among the models becomes evident, with the exception of the model by Stefanakis and Zekentes[5]. However, in this case we suspect a typographical error for the parameter δ which should be 0.61 instead of -0.61. Indeed, we see the main difference among these models in the maximum mobility $\mu_{\max}$.

For the hole mobility less models were proposed with a larger spread in the respective parameters (see Table III). An extreme outlier is the value of $\mu_{\max}$ by Bhatnagar *et al.*[270] that supersedes all remaining values by almost 300 %. Qualitatively, the decrease of the hole mobility, compared to the electron one, starts at a higher doping density (see Fig. 5), i.e., the maximum mobility can be maintained for a longer period of time.

There are bigger uncertainties in regard to the minimum/maximum mobility. For the former Negoro *et al.*[62] pointed out that the value $\mu_{\min} = 16\,\mathrm{cm}^2/(\mathrm{V\,s})$ proposed by Hatakeyama *et al.*[60] is too high. Similarly Stefanakis and Zekentes[5] argues that Schaffer *et al.*[40] overestimates the

TABLE II. Parameters for the Caughey-Thomas model in Eq. (3) used to describe the electron mobility.

ref.	dir	μ_{min}	μ_{max}	μ_0	N_{ref}	δ	γ_{min}	γ_{max}	γ_{ref}	γ_δ	γ_0	γ_{NNref}	N[a]	K[b]	method
		[cm^2/(Vs)]	[cm^2/(Vs)]	[cm^2/(Vs)]	[1/cm^3]	[1]	[1]	[1]	[1]	[1]	[1]	[1]			
[Ruff94][278]	-	20	-	380	4.50×10^{17}	0.45	-	-	-	-	−3	-	-	-	-
[Scha94][40]	⊥	-	947	-	1.94×10^{17}	0.61	-	−2.15	-	-	-	-	S	H	Hall
[Mick98][42]	-	-	1071	-	1.94×10^{17}	0.4	-	-	-	-	-	-	S	C	MC
[Rosc98][279c]	-	40	800	-	4×10^{17}	0.44	-	-	-	-	-	-	D	-	FIT
[Wrig98][137]	-	88	-	970	1.43×10^{17}	1	−0.57	-	2.55	-	−2.7	-	I	-	-
[Mnat01][85d]	-	30	880	-	2×10^{17}	0.67	-	-	-	-	-	-	D	-	FIT
[Mori01][225]	∥	-	1141	-	1.94×10^{17}	0.61	-	-	-	-	-	-	S	C	DIV
[Rosc01][34e]	⊥	40	950	-	2×10^{17}	0.76	−0.5	−2.4	1	-	-	-	D	-	FIT
[Hata03][60]	-	-	954	-	1.28×10^{17}	0.61	-	-	-	-	-	-	I	H	Hall
[Kaga04][81f]	-	-	977	-	1.17×10^{17}	0.49	-	-	-	-	-	-	S	-	FIT
[Adac05][13]	-	-	1400	-	1×10^{17}	0.5	-	-	-	-	-	-	I	-	-
[Bala05][280]	-	40	950	-	2×10^{17}	0.73	-	−2.4	-	-	-	−0.76	-	-	-
[Bhat05][270]	-	27.87	946.97	-	1.75×10^{17}	0.73	-	−2.3	−3.8	-	-	-	-	-	-
[Werb07][154]	-	33	771	-	2×10^{17}	0.76	-	-	-	-	-	-	D	C	DIV
[Cha08][47]	-	-	950	-	1.90×10^{17}	0.6	1	−2.15	-	-	-	0.05	D	-	-
[Habi11][176g]	-	40	-	910	2×10^{17}	0.76	−1.538	-	0.75	0.722	−2.397	-	S	-	FIT
[Hata13][49h]	-	5	1010	-	1.25×10^{17}	0.65	−0.57	−2.6	2.4	−0.146	-	-	S	-	FIT
[Stef14][5i]	⊥	28	950	-	1.94×10^{17}	0.61[j]	-	−2.4	-	-	-	0.73	I	-	FIT
[Shar15][51]	∥	40	947	-	1.94×10^{17}	0.61	−0.5	−2.9	-	-	-	2.4	S	C	DIV
[Arva17][52]	-	40	950	-	1.94×10^{17}	0.61	−1.536	−2.4	-	-	-	-	D	-	-
[Vasi17][39]	-	20	950	-	2×10^{17}	0.8	-	-	-	-	-	-	D	H	Hall
[Loph18][90]	⊥	40	910	-	2×10^{17}	0.76	−1.536	−2.4	0.75	0.722	-	-	-	-	-
	∥	40	1100	-	2×10^{17}	0.76	−1.536	−2.4	0.75	0.722	-	-	-	-	-
[Ishi21][16]	⊥	40	1010	-	2.4×10^{17}	0.7	-	-	-	-	−2.58	-	D	H	Hall
	∥	60	1180	-	2.3×10^{17}	0.74	-	-	-	-	−2.67	-	D	H	Hall
[Rao22][281]	-	40	950	-	2×10^{17}	0.76	−0.5	−2.15	-	-	-	−0.76	I	-	-
[Ishi23][57]	⊥	40	-	1000	2.2×10^{17}	0.68	−0.7	-	-	-	−2.9	−2.5	D	H	Hall
	∥	20	-	1240	2×10^{17}	0.64	0.3	-	-	-	−3.2	−2.7	D	H	Hall

[a] meaning of N: doping (D), ionized (I), sum of all dopants (S), intrinsic (N)

[b] type of mobility: Hall (H), conductivity (C)

[c] fitted to[282]

[d] fitted to[40]

[e] fitted to[40,42,139,144,283,284]

[f] fitted to[21,40,65,166,172,283]

[g] fitted to[40,66,283,284]

[h] fitted to[166]

[i] fitted to[15,17,144,285]

[j] In the paper $\delta = -0.61$ was stated. This did, however, not fit the shown plots

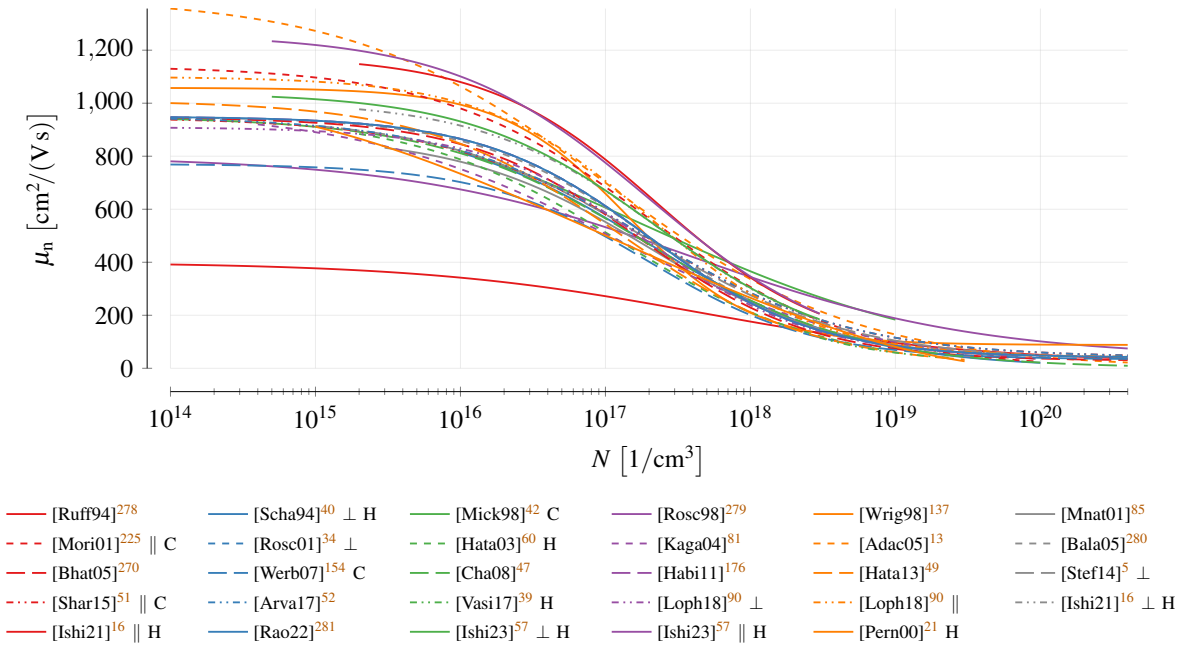

FIG. 4. Electron mobility approximations by the Caughey-Thomas model in Eq. (3) at $T = 300\,\mathrm{K}$. The models are only shown in the region used for characterization.

hole mobility at high doping values, although the latest studies again indicate a value larger than zero. Exceptional in this regard is the very large value of Wright *et al.* [137] that even exceeded some maximum mobility. $\mu_{\max}$ also show variations in the range of 75–140 $\mathrm{cm}^2/(\mathrm{V\,s})$.

Besides Eq. (3) we also found a more direct modeling of the mobility as shown in Eq. (26)[9,10]. According to the authors these expressions are, however, based on Ruff, Mitlehner, and Helbig [278] which only contains values on 6H-SiC.

$$\begin{aligned} \mu_n &= \frac{4.05\times10^{13} + 20N_D^{0.61}}{3.55\times10^{10} + N_D^{0.61}} \\ \mu_p &= \frac{4.05\times10^{13} + 10N_A^{0.65}}{3.3\times10^{11} + N_A^{0.65}} \end{aligned} \tag{26}$$

A different simplified fitting was proposed Pernot *et al.* [21] who fitted the electron Hall mobility to the free electron density n as shown in Eq. (27).

$$\mu_H = -39\,000 + 7436\log(n) - 450.5\log^2(n) + 8.81\log^3(n) \tag{27}$$

Some authors also investigated the impact of compensation on the mobility. Pernot, Contreras, and Camassel [15] fitted the Hall mobility using the logarithmic doping concentration for non-compensated (see Eq. (28)) and weakly-compensated (see Eq. (29)) devices. In the graphical

TABLE III. Parameters for the Caughey-Thomas model in Eq. (3) used to describe the hole mobility.

ref.	dir	μ_{min}	μ_{max}	μ_0	N_{ref}	δ	γ_{min}	γ_{max}	γ_{ref}	γ_δ	γ_0	γ_{NNref}	N[a]	K[b]	method
		$[cm^2/(Vs)]$	$[cm^2/(Vs)]$	$[cm^2/(Vs)]$	$[1/cm^3]$	[1]	[1]	[1]	[1]	[1]	[1]	[1]			
[Ruff94][278]	-	5	-	70	1×10^{19}	0.5	-	-	-	-	−3	-	-	-	-
[Scha94][40]	⊥	15.9	124	-	1.76×10^{19}	0.34	-	-	-	-	-	-	S	H	Hall
[Wrig98][137]	-	74	-	43	1.43×10^{17}	1	−0.57	-	2.55	-	−2.7	-	I	-	-
[Mnat01][85c]	-	33	117	-	1×10^{19}	0.5	-	-	-	-	-	-	D	-	FIT
[Hata03][60]	-	15.9	120	-	1.80×10^{18}	0.65	-	-	-	-	-	-	I	H	Hall
[Mats04][82]	-	37.6	106	-	2.97×10^{18}	0.356	-	-	-	-	-	-	S	H	Hall
[Bala05][280]	-	53.3	105.4	-	2.20×10^{18}	0.7	-	−2.1	-	-	-	-	-	-	-
[Bhat05][270]	-	26.1	401.87	-	1.04×10^{18}	0.7	-	−2.3	−3.8	-	-	-	-	-	-
[Werb07][154]	-	10	-	81	1×10^{19}	0.5	-	-	-	-	-	-	D	C	DIV
[Cha08][47]	-	16	140	-	1.70×10^{19}	0.34	−1.6	−2.14	-	-	-	0.17	D	-	-
[Koiz09][17d]	-	-	114.1	-	5.38×10^{18}	0.66	-	−2.1	-	−0.35	-	2.44	D	H	Hall
[Habi11][176e]	-	40	-	82	6.30×10^{18}	0.55	−1.538	-	0.75	0.722	−2.2397	-	S	-	FIT
[Hata13][49f]	-	-	113.5	-	2.40×10^{18}	0.69	−0.57	−2.6	2.9	−0.2	-	-	S	-	FIT
[Stef14][5g]	⊥	-	114	-	5.38×10^{18}	0.66	-	−2.72	-	−0.35	-	2.44	I	-	FIT
[Liau15][50]	-	-	75	-	2×10^{19}	0.7	-	-	-	-	-	-	D	C	LTPL
[Shar15][51]	∥	15.9	124	-	1.76×10^{19}	0.34	−0.5	−2.9	-	-	-	2.3	S	C	DIV
[Loph18][90]	⊥/∥	-	114	-	2.40×10^{18}	0.69	−0.57	−2.6	2.9	−0.2	-	-	-	-	-
[Tana18][54]	-	-	110	-	3×10^{18}	0.6	-	−3	-	-	-	−1.8	D	H	DFT
	-	-	95	-	1×10^{19}	0.7	-	−2.1	-	-	-	−1.5	D	C	DFT
[Rao22][281]	-	15.9	125	-	1.76×10^{19}	0.76	−0.5	−2.15	-	-	-	−0.76	I	-	-
[Ishi24][58]	⊥	20	-	74	6.2×10^{18}	0.72	−2.2	-	-	-	−2.3	−0.9	D	H	Hall
	∥	20	-	63	6.4×10^{18}	0.83	−2.2	-	-	-	−2.3	−0.9	D	H	Hall

[a] meaning of N: doping (D), ionized (I), sum of all dopants (S), intrinsic (N)

[b] type of mobility: Hall (H), conductivity (C)

[c] fitted to[40]

[d] fitting done by Stefanakis and Zekentes [5]

[e] fitted to[40,66,283,284]

[f] fitted to[166]

[g] fitted to[15,17,144,285]

[h] In the paper $\delta = -0.61$ was stated. This did, however, not fit the shown plots

representation we only show the former case (denoted by NC), since the latter results in negative

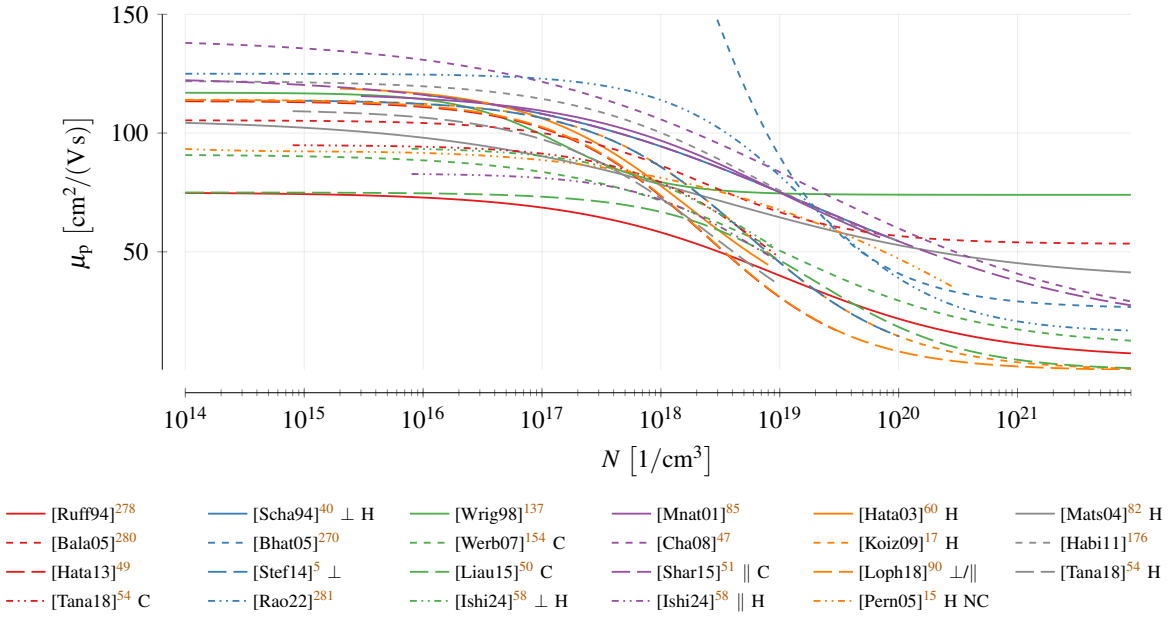

FIG. 5. Hole mobility approximations by the Caughey-Thomas model in Eq. (3) at $T = 300\,\mathrm{K}$. The models are only shown in the region used for characterization.

TABLE IV. Parameters for the model in Eq. (7).

ref	mob.	μ_{min}	μ_{min2}	N_{ref}	δ	μ_1	N_{ref2}	κ
		[cm^2/(Vs)]	[cm^2/(Vs)]	[1/cm^3]	[1]	[cm^2/(Vs)]	[1/cm^3]	[1]
[Zhan18][72]	μ_n	88	0	5×10^{18}	1	43.4	3.43×10^{20}	2
	μ_p	44	0	5×10^{19}	1	29	6.1×10^{20}	2

mobility values. Note that we used $n = N$ and $N_A = N$ for the plots.

$$\begin{aligned}\text{non-compensated: } \sigma R_H(292\,\mathrm{K}) &= 2964.3 - 648.72\log(N_A) + 53.393\log^2(N_A) \\ &\quad -1.8717\log^3(N_A) + 0.002\,296\log^4(N_A) \qquad (28)\\ \text{weakly-compensated: } \sigma R_H(292\,\mathrm{K}) &= 24\,617 - 5982\log(N_A) + 536.12\log^2(N_A) \\ &\quad -21.151\log^3(N_A) + 0.309\,37\log^4(N_A) \qquad (29)\end{aligned}$$

Zhang and You[72] used the Masetti model introduced in Eq. (7) with the parameters shown in Table IV. The additional reduction at doping densities around $10^{20}/\mathrm{cm}^3$ are very well visible. Since no values for μ_{max} were provided we used $950\,\mathrm{cm}^2/(\mathrm{Vs})$ for electrons and $80\,\mathrm{cm}^2/(\mathrm{Vs})$ for holes.

b. Temp Dependency We found various publications that provide detailed in information on the change of the Hall mobility[15–17,21,22,27,28,40,54,57,58,65,66,74,76,78,81,82,84,114,117,120,121,143,144,158,161–169,171,172,

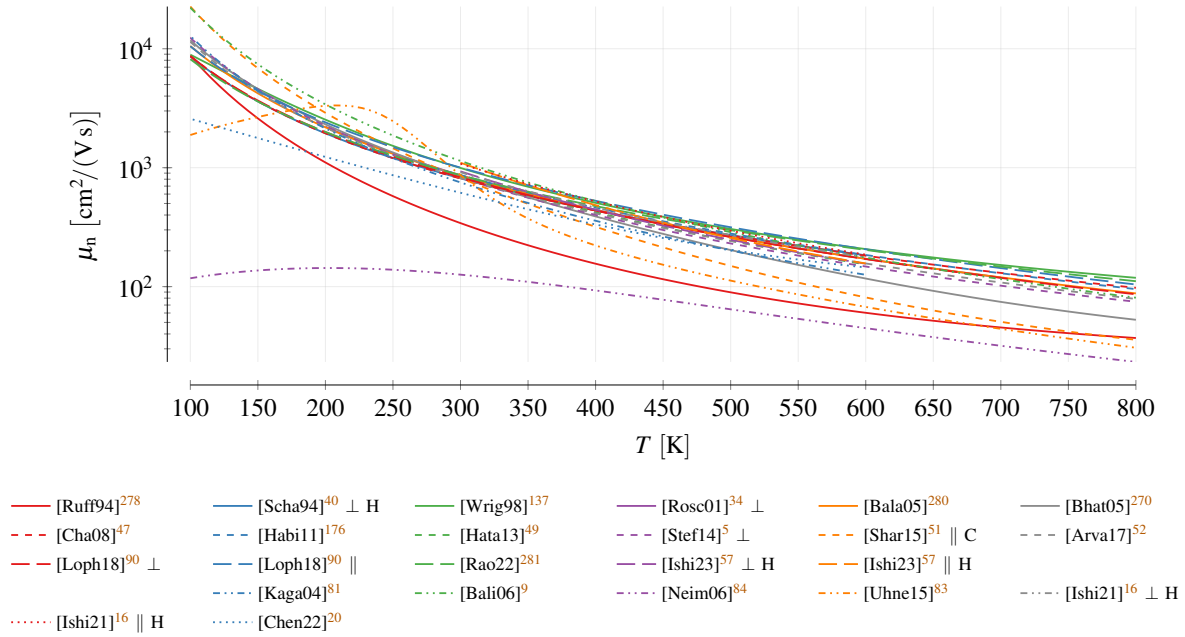

FIG. 6. Description of the electron mobility with varying temperature according to Eq. (3) for a doping of $1 \times 10^{16}/\mathrm{cm}^3$. The dash-dot-dotted lines are based on deviating descriptions (see text).

as well as the conductivity mobility[24,50,79,80,139,142] with varying temperature.

For electrons the fitting parameters for Eq. (3) (see Table II) show lots of deviations. In some cases not even the sign of the parameters is the same for all models. In a graphical representation for a fixed value of $N = 1 \times 10^{16}/\mathrm{cm}^3$ some deviations are visible (see Fig. 6). For low temperatures almost all models agree on high mobilities that further increase with decreasing temperature. This contradicts, however, the increasing impact of impurity scattering, that is only covered by the models proposed by Uhnevionak [83] and Neimontas *et al.* [84]. Note that the latter describes the electron mobility in heavily p-doped material (so the minority mobility), which explains the lower values. An increase at low temperatures was also reported by Götz *et al.* [65] who attributed it to impurity limited mobility and the decrease due to phonon limited mobilities. This also corresponds to the majority of measurements we saw, implying once more that the temperature dependency is only valid in a very narrow range for the majority of the available models.

Others observe a dependency of $T^{-2.1}$ to $T^{-2.5}$ instead of the expected $T^{-1.5}$[76,166,167]. The temperature dependency even shows anisotropy. Schaffer *et al.* [40] proposed a temperature scaling parallel to the c-axis of $T^{-2.4}$ and perpendicular $T^{-2.15}$ above 200 K. Below that value they get $T^{-1.2}$ (parallel) and $T^{-1.18}$ (perpendicular). Ishikawa *et al.* [16] investigated the temperature dependency for three differing dopings, seeing a significant absolute decrease with increasing doping

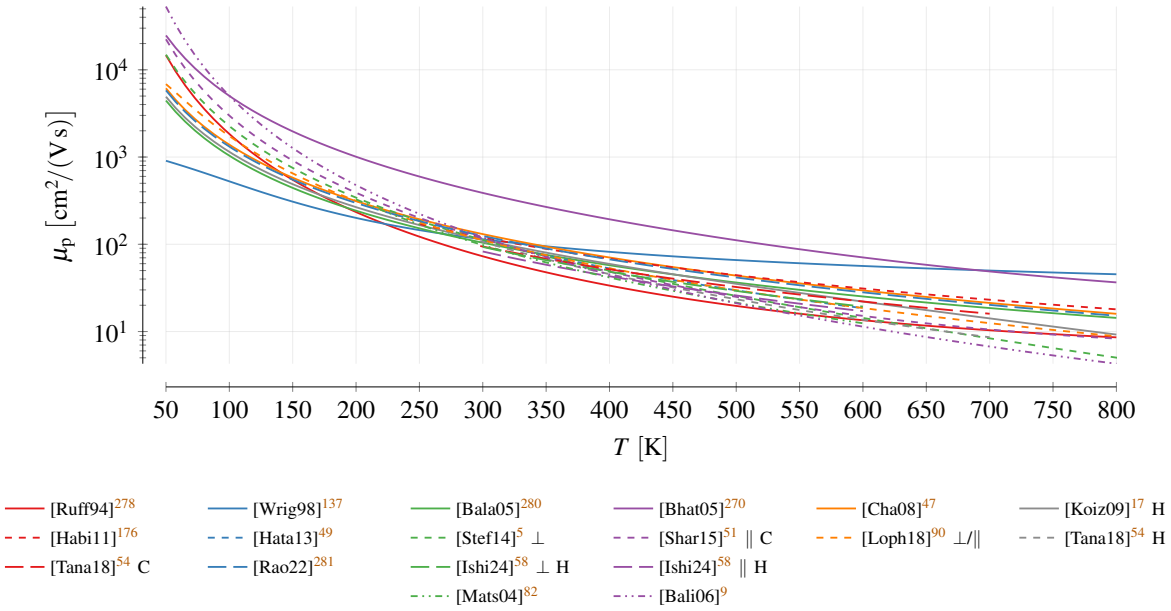

FIG. 7. Description of the hole mobility with varying temperature according to Eq. (3) for a doping of $1 \times 10^{16}/\mathrm{cm}^3$.

concentration and an anisotropy[58]. In[16] the whole mobility is scaled by $T^{-\beta}$ whereat β is doping dependent. In Fig. 6 we chose $\beta = -2.38$ perp. to the c-axis and $\beta = -2.54$ parallel to it which corresponds to measurements on a doping concentration of $N_\mathrm{D} = 3.6 \times 10^{16}/\mathrm{cm}^3$.

For holes the fitting parameters for Eq. (3) (see Table III) show the same inconsistencies as the electron data. The graphical representation reveals a much higher agreement among the single models (see Fig. 7). All models predict a continuous decrease with increasing temperature.

Buono[48] argued that the temperature dependency μ_max for both charge carriers with $\gamma_\mathrm{max} = -2.15$ is smaller than the ideal factor of -1.5 that is expected from lattice scattering. This was believed to be due to non-polar optical-phonon scattering. Lades[19] achieved $-1.8 \geq \gamma_\mathrm{max} \geq -2.2$, which lies between acoustical-mode phonon (-1.5) and optical-mode phonon (-2.5) scattering. Thus they assumed the contribution of other scattering factors contribute less to limit the mobility.

For Eq. 9 and Eq. 10 the parameter values shown in Table V were proposed. Note that in this case the temperature coefficient scales with the doping concentration. Kagamihara *et al.*[81] stated that according to theoretical consideration the temperature parameters are 1.5 for low temperatures and 2.6 for high ones, which is close to β_min (1.54) and β_max (2.62) in their fitting.

In contrast to Eq. (3) also more straightforward model for the temperature dependency of the mobility exist. Cheng, Yang, and Zheng[20] fitted the expression shown in Eq. (30) to the measure-

TABLE V. Parameters for the model in Eq. 9 and Eq. 10.

ref	mob.	β_{min} [1]	β_{max} [1]	N_{p} [1/cm^3]	η [1]	K	method
[Kaga04][81]	μ_{n}	1.54	2.62	1.14×10^{17}	1.35	-	FIT
[Mats04][82]	μ_{p}	2.51	3.04	8.64×10^{17}	0.456	H	Hall

TABLE VI. Parameters for the model in Eq. (12) and Eq. (13).

ref	mob.	μ_{min} [cm^2/(V s)]	μ_{max} [cm^2/(V s)]	N_{ref} [1/cm^3]	δ [1]	γ_{max} [1]	γ_{l} [1]
[Neim06][84]	μ_{n}	100	320	2×10^{17}	-0.67[a]	2.6	0.5

[a] In the paper this value is 0.67 but we changed it to achieve the same results as shown in the paper.

ments of the electron mobility by Schaffer *et al.*[40].

$$\mu_{\text{n}}(T) = 5422 \exp\left(-\frac{T}{128}\right) + 95 \tag{30}$$

In[9,10] simplified equations that just use a constant mobility combined with a temperature scaling have been presented, which are based on a fitting to data from Koizumi, Suda, and Kimoto[17] and a reference to[137].

$$\mu_{\text{n}}(T) = 1140 \exp\left(\frac{T}{300}\right)^{-2.7}, \mu_{\text{p}}(T) = 120 \exp\left(\frac{T}{300}\right)^{-3.4} \tag{31}$$

The model proposed by Uhnevionak[83] shown in Eq. (11) that splits μ_{max} in two parts is also shown in the figure using the parameters $\mu_{\text{max1}} = 500$, $\gamma_{\text{max1}} = -11.6$, $\mu_{\text{max2}} = 450$, $\gamma_{\text{max2}} = -2.74$, $\gamma_{\text{NNref}} = -12.5$ and the remaining parameters according to Roschke and Schwierz[34].

We also plotted the model proposed in Eq. (12) and Eq. (13) with the parameters introduced by Neimontas *et al.*[84] shown in Table VI. These describe the electron mobility in heavily p-doped 4H-SiC.

c. Analysis An investigation of the consistency of 4H-SiC mobility models is challenging. In the sequel we want to highlight the most striking issues we encountered. A more complete listing of all inconsistencies is presented in **??**.

First of all, we were unable to retrace some values[90,280,285,286] back to scientific publications. In other cases references were provided but the presented values could not be found therein[8,90].

Some publications even present multiple models[89,99,196] that contradict each other.

In the case of electrons sometimes different models seem to be mixed, e.g., using the mobility values from one and the temperature scaling from another. Often a combination of the models by Schaffer *et al.*[40] and Roschke and Schwierz[34] were encountered[44,52,87,94,276] (see Fig. 8). These are also the most influential publications, whereat newer studies have barely been adopted in literature. On the positive side almost all references go back to one of the fundamental studies and almost exclusively 4H values are used. The only exception are the values by Ruff, Mitlehner, and Helbig[278], which are, however, also seldomly used.

For holes (see Fig. 9) the majority of the values goes back to a single publication by Schaffer *et al.*[40], whereat, again, newer values do not spread well within the community. We are also unsure about the temperature scaling of the hole mobility in the publications citing[40], which seem to be taken directly from electrons. There are also various occacions[63,96,276,292,293,296] where μ_{max} was interpreted as μ_0, i.e., μ_{min} is not subtracted.

At last we want to investigate two previous reviews on mobility models in greater details, as we encountered problematic parameters that need to be discussed. We begin with the analysis by Stefanakis and Zekentes[5] who investigated six models and fitted a seventh to measurement results for holes. The model denoted as "Reggio Calabria Uni." was cited from Pezzimenti[301] but go back to Schaffer *et al.*[40] for holes and Roschke and Schwierz[34] for electrons. There are also some mistakes with the parameters. δ of the electrons should be 0.76 instead of 0.34, while γ_{NNref} of the holes should be -0.34 instead of -0.76. A similar mistake happened for the values cited from Nawaz[285], where for the electrons $\delta = 0.73$ instead of the stated 0.34 and $\gamma_{\mathrm{NNref}} = -0.76$ instead of 0.73 were proposed. For holes μ_{min} should be $53.3\,\mathrm{cm^2/(V\,s)}$ instead of the stated $15.3\,\mathrm{cm^2/(V\,s)}$. In table 3 and 4 the entries by Bakowski, Gustafsson, and Lindefelt[41] and Brosselard[307] were switched, whereat the then appropriate values for the former are still not fully correct since the temperature scaling is regarding to μ_0 and not μ_{max}. The fitting of γ_{NNref} for the values presented by Koizumi, Suda, and Kimoto[17] is also questionable as the value proposed for N_{ref} is shown in the measurements for 400 K instead of 300 K and for $\gamma_{\mathrm{NNref}} = 2.44$ the value of N_{ref} effectively decreases with rising temperature, although the measurements show the opposite. Finally, we again want to highlight that the value δ for electrons should be 0.61 instead of the proposed -0.61.

The second overview paper was published by Tian *et al.*[6]. Some mistakes happened for the values cited from Nawaz[285], where for the electrons $\delta = 0.73$ instead of the stated 0.34 and

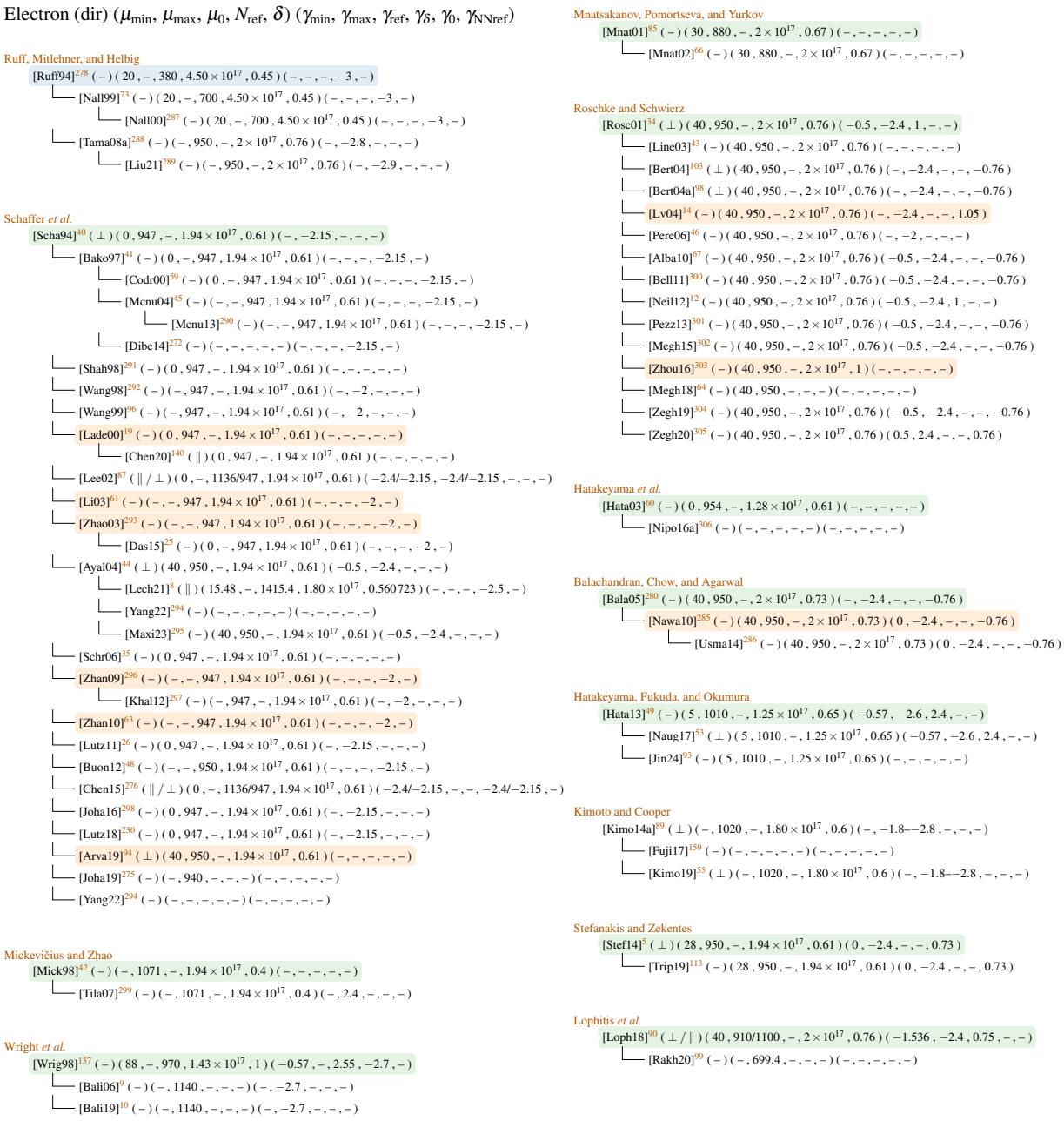

FIG. 8. Reference chain for low field electron mobility models. are fundamental investigations, research not focused on 4H and connections predicted from the used values.

$\gamma_{NNref} = -0.76$ instead of 0.73 were proposed earlier. For holes μ_{min} should be 53.3 $cm^2/(Vs)$ instead of the stated 15.3 $cm^2/(Vs)$. Note that these are the same flaws as discovered in[5]. Despite these variations, this model delivered the best results and was chosen for the simulations. In addition, the maximum mobility for electrons from[48] was changed from 950 $cm^2/(Vs)$ to 947 $cm^2/(Vs)$. The model proposed by Megherbi *et al.*[64] was extended by a temperature scal-

FIG. 9. Reference chain for low field hole mobility models. are fundamental investigations, research not focused on 4H and connections predicted from the used values.

ing, which matches an earlier publication by the same authors[302] without, however, the correct value for γ_{NNref}.

Interesting is also that the origin of the model proposed by Wright[136], which is denoted as "Brosselard" in[5] and "Gustaffson" in[6] could not yet be fully identified.

3. *High-Field Mobility*

While early publications on SiC had to rely on Silicon parameters[278] later many studies about the dependency of the electron resp. hole velocity on varying electric field were published[30,42,55,98,100–102,104,105,128,140,145–149]. These led to various parameters to describe the high-field electron mobility with the model introduced in Eq. (14) (see Table VII). The saturation velocity parallel to the c-axis is lower compared to the perpendicular direction. Hatakeyama *et al.* [308] estimated the ratio based on impact ionization coefficients (see **??**), whereat Hatakeyama, Fukuda, and Okumura[49] achieved that the electron velocity parallel to the c-axis is 60 % of the perpendicular one and 80 % for holes. In the table we also added measurements and simulations that only delivered the saturation velocity without any fitting. Overall the values range from a few $10^6\,\mathrm{V/cm}$ to a few $10^7\,\mathrm{V/cm}$.

The hole saturation velocity is marginally lower than the electron one (see Table VIII). The key difference, clearly, is the amount of conducted investigations. Often the value of the hole saturation velocity is just assumed[52,89] or set equal to the electron one[52,96,99,278,279,301].

As already indicated earlier Monte-Carlo simulations reveal a maximum in the charge carrier velocity, followed by a decrease with increasing field strengths[12,14,42,98,100–106]. While some then achieve a constant value, others report a steadily decreasing velocity. In all these simulation reports, the peak velocity is highlighted, and even denoted as saturation velocity. Nevertheless, other sources see this as a velocity overshoot[12,14,99], but also denote that this effect has yet only be seen in simulations and not in experiments[99].

A graphical representation of the single models for the electron velocity show quite good agreement (see Fig. 10). It can be seen that the first deviations among the model are visible already at a few kV/cm. The mobility starts to change at around $10\,\mathrm{kV/cm}$[10], which is significantly smaller than the $200\,\mathrm{kV/cm}$ proposed by Lophitis *et al.* [90]. We do not explicitely show the results for holes as only a single model could be found.

The description by Lv *et al.* [14] used the model introduced in Eq. (17) with the parameter shown in Eq. (32). Note that we were unable to recreate the plots shown in the paper, which are, considering the provided parameters, not retraceable for us.

$$\begin{aligned} &\mu_0 = 0.17\mu_1\ ,\ \alpha = -1.95\ ,\ \beta = 3 \\ &F_0 = 3.05\times10^4\,\mathrm{V/cm}\ ,\ F_1 = 2.8\times10^5\,\mathrm{V/cm}\ ,\ v_{\mathrm{max}} = 4.8\times10^7\,\mathrm{cm/s} \end{aligned} \tag{32}$$

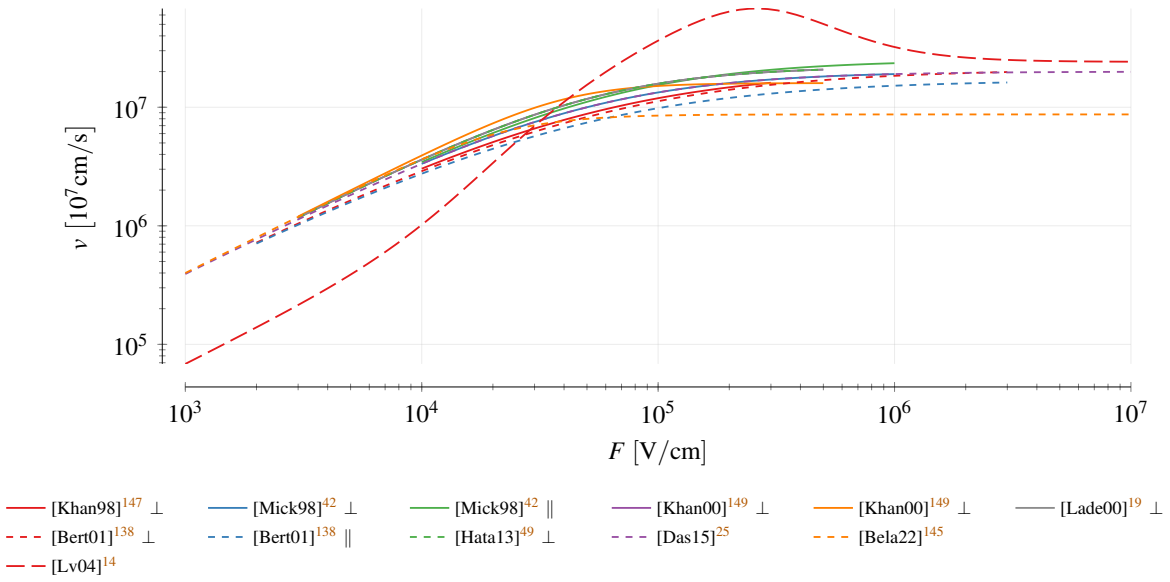

FIG. 10. Electron carrier velocity with varying field for $\mu_{\text{low}} = 400\,\text{cm}^2/(\text{V s})$. Long dashed models describe velocity according to Eq. (17).

In overview listings the electron saturation velocity is dominantly denoted by $2 \times 10^7\,\text{cm/s}$ (see Fig. 11). This popular value was already reported by V. Muench and Pettenpaul [311] for 6H, as pointed out by[147], and then reused for 4H. Nevertheless, later investigations confirmed the validity also for 4H. Slightly lower/higher values are also available but not nearly as prominent. For holes very similar values were proposed (see Fig. 12) but, again, in much less amount.

The temperature dependency of the high-field velocity was measured by Khan and Cooper[147,149] or investigated by simulations[98,103]. Later these results were numerically fitted[19,49]. Note that Lades [19] used a linear fit for the exponent β such that the value published by Khan and Cooper [149] for 620 K could not be perfectly matched (2.2 vs. 2.4).

The results predict a decrease of the saturation velocity with increasing temperature (see Table VII and Table VIII). The values published by Das and Duttagupta [25], however, predict the exact opposite. This is also visible in a graphical representation (see Fig. 13). The values by Roschke and Schwierz [34] and Bertilsson, Harris, and Nilsson [98] were described by the model introduced in Eq. (15) and Eq. (16) with the parameters shown in Table IX, which were referenced by[12,67,96,271].

Finally the reference chain (see Fig. 14 for electrons and Fig. 15 for holes) clearly shows that many different publications are referenced in literature.

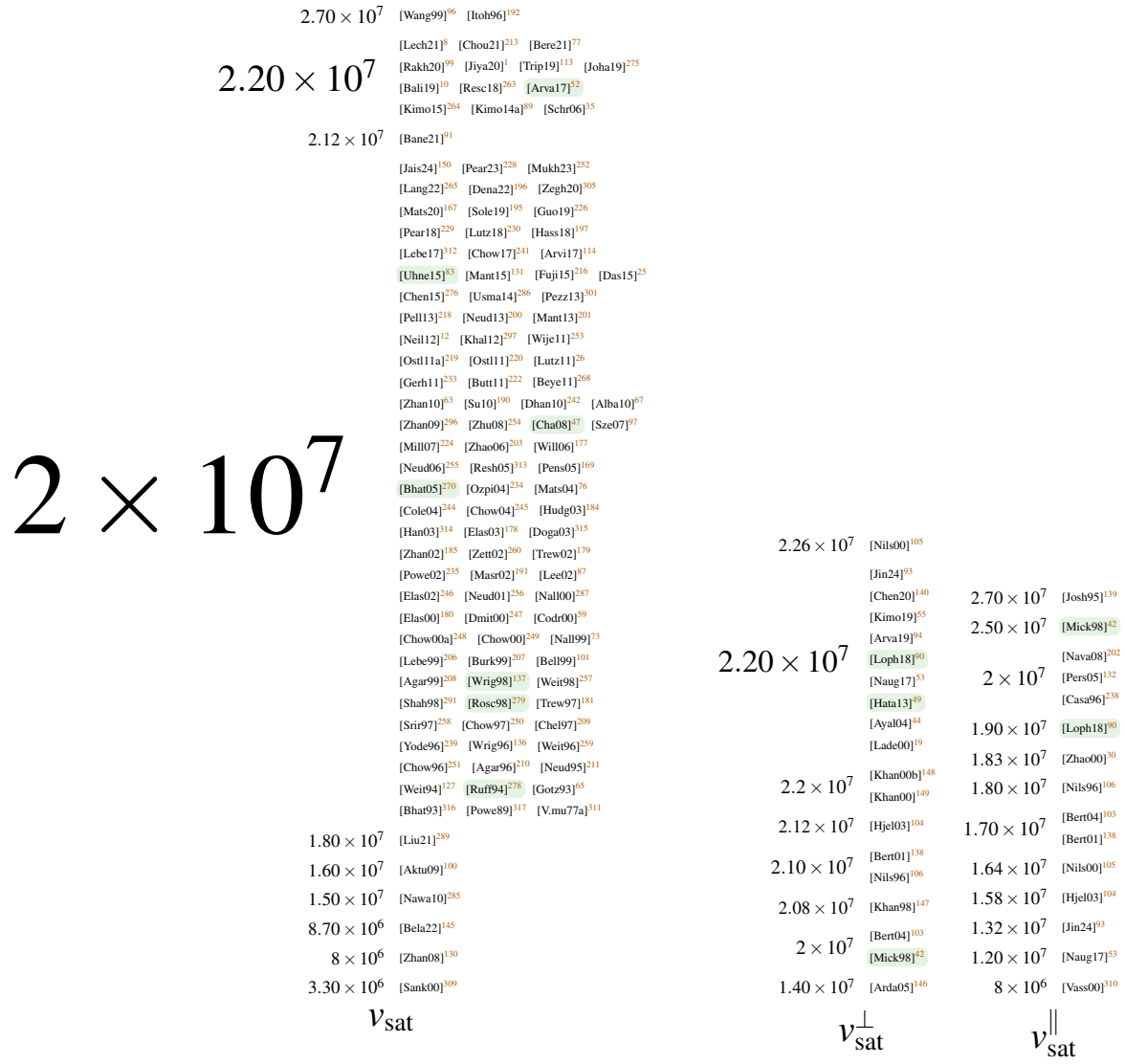

FIG. 11. Electron saturation velocity values used in literature. are fundamental investigations.

4. Carrier-Carrier Scattering

The only investigation of carrier-carrier scattering in 4H-SiC we found was conducted by Lades[19], who started from the parameters of Eq. (19) for Silicon and scaled them until the results fit to 4H-SiC measurements. In this fashion the values shown in Eq. (33) were achieved, which are already reused at various occasions[35,44,113]

$$D = 6.9 \times 10^{20}/(\mathrm{cm\,V\,s})\ ,\ F = 7.452 \times 10^{13}/\mathrm{cm}^2 \tag{33}$$

In addition Onoda *et al.*[112] proposed values for 6H. Bhatnagar *et al.*[270] proposed separate values for electrons and holes but used an equation that was developed by Dorkel and Leturcq[110]

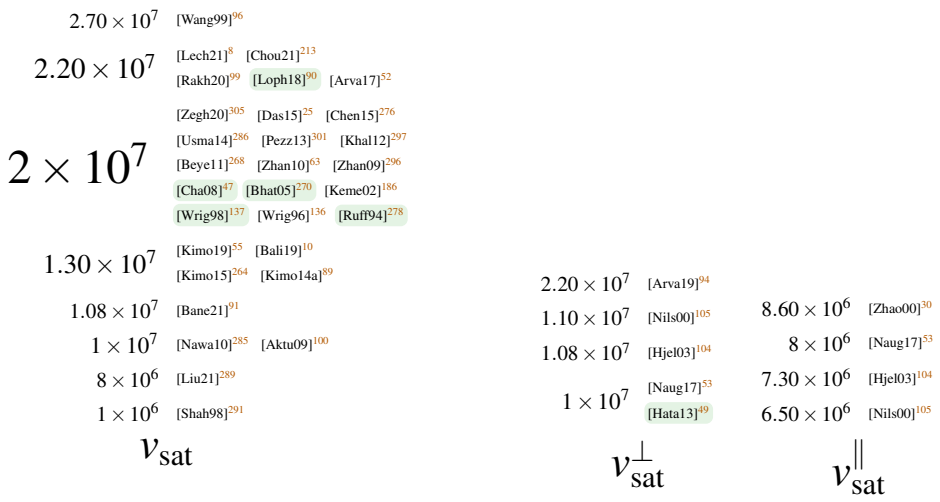

FIG. 12. Hole saturation velocity values used in literature. are fundamental investigations.

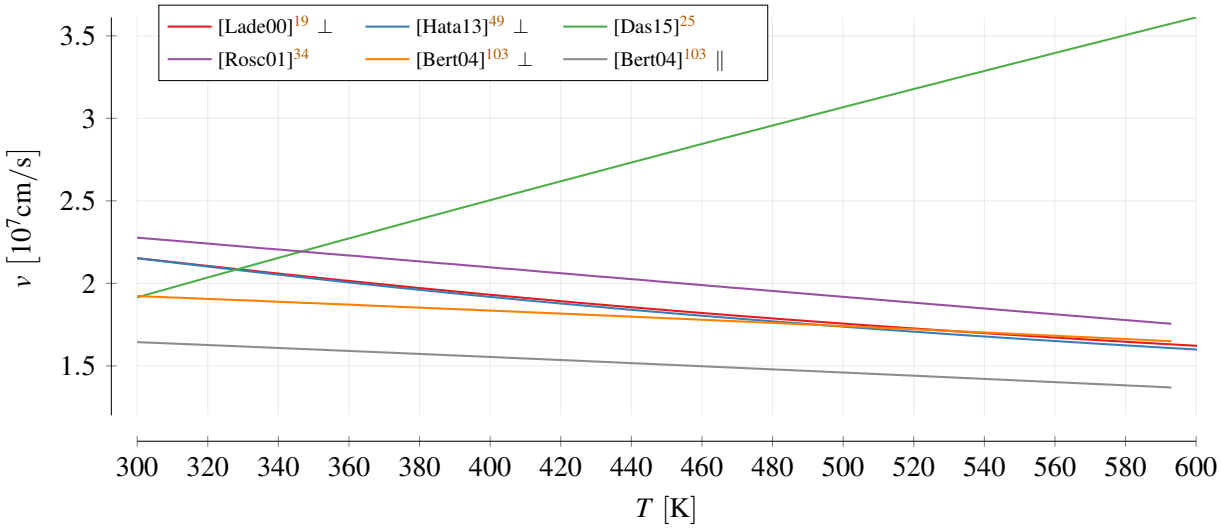

FIG. 13. Temperature dependency of electron velocity for $F = 10^6\,\mathrm{V/cm}$ and $\mu_{\mathrm{low}} = 450\,\mathrm{cm^2/(V\,s)}$.

for impurity scattering. Lechner[8] referenced the values by Fletcher[318], which are, however, for Silicon.

FIG. 14. High-field mobility reference chain for electrons.

TABLE VII. High field mobility parameters in Eq. (14) for electrons.

ref.	v_{sat} [cm/s]	$v_{sat}^{\perp}$ [cm/s]	$v_{sat}^{\parallel}$ [cm/s]	γ_{sat} [1]	β [1]	γ_{β} [1]	T_{sat} [K]	K[a]	method
[Ruff94][278][b]	2×10^7	-	-	-	2	-	-	-	-
[Josh95][139]	-	-	2.70×10^7	-	-	-	-	C	MC
[Nils96][106]	-	2.10×10^7	1.80×10^7	-	-	-	-	C	MC
[Khan98][147]	-	2.08×10^7	-	-	0.825	-	-	C	NPC
[Mick98][42]	-	2×10^7	2.50×10^7	-	1	-	-	C	MC
[Khan00][149]	-	2.2×10^7	-	-	1.2	-	296	C	NPC
	-	1.6×10^7	-	-	2.2	-	593	C	NPC
[Lade00][19][c]	-	2.20×10^7	-	-0.44	1.2	1	-	-	FIT
[Nils00][105]	-	2.26×10^7	1.64×10^7	-	-	-	-	C	MC
[Sank00][309]	3.30×10^6	-	-	-	-	-	-	C	BIV
[Vass00][310]	-	-	8×10^6	-	-	-	300	C	DIV
	-	-	7.5×10^6	-	-	-	460	C	DIV
[Zhao00][30]	-	-	1.83×10^7	-	-	-	-	C	MCP
[Bert01][138]	-	2.10×10^7	1.70×10^7	-	0.84/1.1[d]	-	-	C	MC
[Hjel03][104]	-	2.12×10^7	1.58×10^7	-	-	-	-	C	EPM
[Bert04][103]	-	2×10^7	1.70×10^7	-	-	-	-	C	MC
[Arda05][146]	-	1.40×10^7	-	-	-	-	-	C	NPC
[Aktu09][100]	1.60×10^7	-	-	-	-	-	-	C	MC DFT-DOS
[Hata13][49][e]	-	2.20×10^7	-	-0.46	1.20	0.88	-	-	FIT
[Das15][25]	2×10^7	-	-	0.87	1	0.66	-	-	-
[Bela22][145]	8.70×10^6	-	-	-	2	-	-	C	CCh
[Jais24][150]	2×10^7	-	-	-	-	-	-	C	DIV

[a] type of mobility: Hall (H), conductivity (C)
[b] β taken from Silicon
[c] fitted to[149]
[d] values of β $\perp$ / $\parallel$ to c-axis
[e] fitted to[19,149]

TABLE VIII. High field mobility parameters in Eq. (14) for holes.

ref.	v_{sat} [cm/s]	$v_{sat}^{\perp}$ [cm/s]	$v_{sat}^{\parallel}$ [cm/s]	γ_{sat} [1]	β [1]	γ_{β} [1]	T_{sat} [K]	K[a]	method
[Ruff94][278b]	2×10^7	-	-	-	-	-	-	-	-
[Nils00][105]	-	1.10×10^7	6.50×10^6	-	-	-	-	C	MC
[Zhao00][30]	-	-	8.60×10^6	-	-	-	-	C	MCP
[Hjel03][104]	-	1.08×10^7	7.30×10^6	-	-	-	-	C	EPM
[Aktu09][100]	1×10^7	-	-	-	-	-	-	C	MC DFT-DOS
[Kimo14a][89]	1.30×10^7	-	-	-	-	-	-	-	-
[Das15][25]	2×10^7	-	-	0.52	1.213	0.17	-	-	-

[a] type of mobility: Hall (H), conductivity (C)

[b] v_{sat} set equal to electron saturation velocity

TABLE IX. Model parameters for temperature dependent carrier velocity in Eq. (15) and Eq. (16).

ref.	dir	v_{max} [cm/s]	d [1]	β_0 [1]	T_{ref} [K]	a [1]	b [K]	c [1/K]
[Rosc01][34a]	-	4.77×10^7	0.6	0.816	327	4.27×10^{-2}	98.4	0
[Bert04a][98b]	$\perp$	2.77×10^7	0.23	0.6	0	0	∞	10^{-3}
	$\parallel$	2.55×10^7	0.3	1.01	0	0	∞	3×10^{-4}

[a] fitted to[106,149]

[b] fitted to simulations by Nilsson, Sannemo, and Petersson [106]

FIG. 15. High-field mobility reference chain for holes.

REFERENCES

[1]I. N. Jiya and R. Gouws, Micromachines **11**, 1116 (2020).

[2]C. Raynaud, D.-M. Nguyen, N. Dheilly, D. Tournier, P. Brosselard, M. Lazar, and D. Planson, physica status solidi (a) **206**, 2273 (2009).

[3]D. Stefanakis, N. Makris, K. Zekentes, and D. Tassis, IEEE Transactions on Electron Devices **68**, 2582 (2021).

[4]V. I. Sankin, Semiconductors **36**, 717 (2002).

[5]D. Stefanakis and K. Zekentes, Microelectronic Engineering **116**, 65 (2014).

[6]K. Tian, J. Xia, K. Elgammal, A. Schöner, W. Kaplan, R. Karhu, J. Ul-Hassan, and A. Hallén, Materials Science in Semiconductor Processing **115**, 105097 (2020).

[7]M. J. Marinella, D. K. Schroder, G. Chung, M. J. Loboda, T. Isaacs-Smith, and J. R. Williams, IEEE Transactions on Electron Devices **57**, 1910 (2010).

[8]B. Lechner, *Behaviour of 4H-SiC Power Semiconductor Devices under Extreme Operating Conditions*, Ph.D. thesis, Technische Universität München (2021).

[9]B. J. Baliga, *Silicon Carbide Power Devices* (WORLD SCIENTIFIC, 2006).

[10]B. J. Baliga, *Fundamentals of Power Semiconductor Devices* (Springer International Publishing, Cham, 2019).

[11]C. Darmody and N. Goldsman, Journal of Applied Physics **126**, 145701 (2019).

[12]I. Neila Inglesias, "APPLYING NUMERICAL SIMULATION TO MODELS SiC SEMICONDUCTOR DEVICES," (2012).

[13]S. Adachi, *Properties of Group-IV, III-V and II-VI Semiconductors* (John Wiley, Chichester, England, 2005).

[14]H. Lv, Y. Zhang, Y. Zhang, and L.-A. Yang, IEEE Transactions on Electron Devices **51**, 1065 (2004).

[15]J. Pernot, S. Contreras, and J. Camassel, Journal of Applied Physics **98**, 023706 (2005).

[16]R. Ishikawa, M. Hara, H. Tanaka, M. Kaneko, and T. Kimoto, Applied Physics Express **14**, 061005 (2021).

[17]A. Koizumi, J. Suda, and T. Kimoto, Journal of Applied Physics **106**, 013716 (2009).

[18]N. Kaji, H. Niwa, J. Suda, and T. Kimoto, IEEE Transactions on Electron Devices **62**, 374 (2015).

[19]M. Lades, *Modeling and Simulation of Wide Bandgap Semiconductor Devices: 4H/6H-SiC*,

Ph.D. thesis, Technische Universität München (2000).

[20]L. Cheng, J.-Y. Yang, and W. Zheng, ACS Applied Electronic Materials **4**, 4140 (2022).

[21]J. Pernot, S. Contreras, J. Camassel, J. L. Robert, W. Zawadzki, E. Neyret, and L. Di Cioccio, Applied Physics Letters **77**, 4359 (2000).

[22]J. Pernot, W. Zawadzki, S. Contreras, J. L. Robert, E. Neyret, and L. Di Cioccio, Journal of Applied Physics **90**, 1869 (2001).

[23]S. Selberherr, *Analysis and Simulation of Semiconductor Devices* (Springer Vienna, Vienna, 1984).

[24]B. K. Meyer, D. M. Hofmann, D. Volm, W. M. Chen, N. T. Son, and E. Janzén, Physical Review B **61**, 4844 (2000).

[25]A. Das and S. P. Duttagupta, Radiation Protection Dosimetry **167**, 443 (2015).

[26]J. Lutz, H. Schlangenotto, U. Scheuermann, and R. De Doncker, *Semiconductor Power Devices: Physics, Characteristics, Reliability* (Springer Berlin Heidelberg, Berlin, Heidelberg, 2011).

[27]H. Iwata, K. M. Itoh, and G. Pensl, Journal of Applied Physics **88**, 1956 (2000).

[28]H. Iwata and K. M. Itoh, Journal of Applied Physics **89**, 6228 (2001).

[29]H. Harima, S.-i. Nakashima, and T. Uemura, Journal of Applied Physics **78**, 1996 (1995).

[30]J. H. Zhao, V. Gruzinskis, Y. Luo, M. Weiner, M. Pan, P. Shiktorov, and E. Starikov, Semiconductor Science and Technology **15**, 1093 (2000).

[31]H. Matsuura, A. Takeshita, T. Imamura, K. Takano, K. Okuda, A. Hidaka, S. Ji, K. Eto, K. Kojima, T. Kato, S. Yoshida, and H. Okumura, Applied Physics Express **11**, 101302 (2018).

[32]Y. Kajikawa, Journal of Electronic Materials **50**, 1247 (2021).

[33]H. Kim, Transactions on Electrical and Electronic Materials **25**, 141 (2024).

[34]M. Roschke and F. Schwierz, IEEE Transactions on Electron Devices **48**, 1442 (2001).

[35]D. Schröder, *Leistungselektronische Bauelemente* (Springer Berlin Heidelberg, Berlin, Heidelberg, 2006).

[36]D. Caughey and R. Thomas, Proceedings of the IEEE **55**, 2192 (1967).

[37]N. Arora, J. Hauser, and D. Roulston, IEEE Transactions on Electron Devices **29**, 292 (1982).

[38]M. Huang, N. Goldsman, C.-H. Chang, I. Mayergoyz, J. M. McGarrity, and D. Woolard, Journal of Applied Physics **84**, 2065 (1998).

[39]K. Vasilevskiy, S. K. Roy, N. Wood, A. B. Horsfall, and N. G. Wright, Materials Science Forum **897**, 254 (2017).

[40]W. J. Schaffer, G. H. Negley, K. G. Irvine, and J. W. Palmour, MRS Proceedings **339**, 595 (1994).

[41]M. Bakowski, U. Gustafsson, and U. Lindefelt, physica status solidi (a) **162**, 421 (1997).

[42]R. Mickevičius and J. H. Zhao, Journal of Applied Physics **83**, 3161 (1998).

[43]H. Linewih, S. Dimitrijev, and K. Y. Cheong, Microelectronics Reliability **43**, 405 (2003).

[44]T. Ayalew, *SiC Semiconductor Devices Technology, Modeling, and Simulation*, Ph.D. thesis, TU Wien (2004).

[45]T. McNutt, A. Hefner, H. Mantooth, J. Duliere, D. Berning, and R. Singh, IEEE Transactions on Power Electronics **19**, 573 (2004).

[46]A. Pérez-Tomás, P. Brosselard, P. Godignon, J. Millán, N. Mestres, M. R. Jennings, J. A. Covington, and P. A. Mawby, Journal of Applied Physics **100**, 114508 (2006).

[47]H.-Y. Cha and P. M. Sandvik, Japanese Journal of Applied Physics **47**, 5423 (2008).

[48]B. Buono, *Simulation and Characterization of Silicon Carbide Power Bipolar Junction Transistors*, Ph.D. thesis, KTH Royal Institute of Technology (2012).

[49]T. Hatakeyama, K. Fukuda, and H. Okumura, IEEE Transactions on Electron Devices **60**, 613 (2013).

[50]G. Liaugaudas, D. Dargis, P. Kwasnicki, H. Peyre, R. Arvinte, S. Juillaguet, M. Zielinski, and K. Jarašiūnas, Materials Science Forum **821–823**, 249 (2015).

[51]R. K. Sharma, P. Hazdra, and S. Popelka, IEEE Transactions on Nuclear Science **62**, 534 (2015).

[52]A. Arvanitopoulos, N. Lophitis, S. Perkins, K. N. Gyftakis, M. Belanche Guadas, and M. Antoniou, in *2017 IEEE 11th International Symposium on Diagnostics for Electrical Machines, Power Electronics and Drives (SDEMPED)* (IEEE, Tinos, Greece, 2017) pp. 565–571.

[53]A. Naugarhiya, P. Wakhradkar, P. N. Kondekar, G. C. Patil, and R. M. Patrikar, Journal of Computational Electronics **16**, 190 (2017).

[54]H. Tanaka, S. Asada, T. Kimoto, and J. Suda, Journal of Applied Physics **123**, 245704 (2018).

[55]T. Kimoto, in *Wide Bandgap Semiconductor Power Devices* (Elsevier, 2019) pp. 21–42.

[56]Y. Huang, R. Wang, Y. Zhang, D. Yang, and X. Pi, Journal of Applied Physics **131**, 185703 (2022).

[57]R. Ishikawa, H. Tanaka, M. Kaneko, and T. Kimoto, physica status solidi (b) **260**, 2300275 (2023).

[58]R. Ishikawa, H. Tanaka, M. Kaneko, and T. Kimoto, Journal of Applied Physics **135**, 075704

(2024).

[59]C. Codreanu, M. Avram, E. Carbunescu, and E. Iliescu, Materials Science in Semiconductor Processing **3**, 137 (2000).

[60]T. Hatakeyama, T. Watanabe, M. Kushibe, K. Kojima, S. Imai, T. Suzuki, T. Shinohe, T. Tanaka, and K. Arai, Materials Science Forum **433–436**, 443 (2003).

[61]X. Li, Y. Luo, L. Fursin, J. Zhao, M. Pan, P. Alexandrov, and M. Weiner, Solid-State Electronics **47**, 233 (2003).

[62]Y. Negoro, T. Kimoto, H. Matsunami, F. Schmid, and G. Pensl, Journal of Applied Physics **96**, 4916 (2004).

[63]Y.-R. Zhang, B. Zhang, Z.-J. Li, and X.-C. Deng, Chinese Physics B **19**, 067102 (2010).

[64]M. L. Megherbi, F. Pezzimenti, L. Dehimi, M. A. Saadoune, and F. G. Della Corte, IEEE Transactions on Electron Devices **65**, 3371 (2018).

[65]W. Götz, A. Schöner, G. Pensl, W. Suttrop, W. J. Choyke, R. Stein, and S. Leibenzeder, Journal of Applied Physics **73**, 3332 (1993).

[66]T. T. Mnatsakanov, M. E. Levinshtein, L. I. Pomortseva, and S. N. Yurkov, Semiconductor Science and Technology **17**, 974 (2002).

[67]L. F. Albanese, *Characterization, Modeling and Simulation of 4H-SiC Power Diodes*, Ph.D. thesis, UniversitàdegliStudidiSalerno (2010).

[68]S. N. Mohammad, A. V. Bemis, R. L. Carter, and R. B. Renbeck, Solid-State Electronics **36**, 1677 (1993).

[69]M. Sotoodeh, A. H. Khalid, and A. A. Rezazadeh, Journal of Applied Physics **87**, 2890 (2000).

[70]G. Masetti, M. Severi, and S. Solmi, IEEE Transactions on Electron Devices **30**, 764 (1983).

[71]C. Lombardi, S. Manzini, A. Saporito, and M. Vanzi, IEEE Transactions on Computer-Aided Design of Integrated Circuits and Systems **7**, 1164 (1988).

[72]X. Zhang and N. You, in *2018 IEEE 3rd International Conference on Integrated Circuits and Microsystems (ICICM)* (IEEE, Shanghai, 2018) pp. 60–63.

[73]F. Nallet, D. Planson, K. Isoird, M. Locatelli, and J. Chante, in *CAS '99 Proceedings. 1999 International Semiconductor Conference (Cat. No.99TH8389)*, Vol. 1 (IEEE, Sinaia, Romania, 1999) pp. 195–198.

[74]M. Rambach, L. Frey, A. J. Bauer, and H. Ryssel, Materials Science Forum **527–529**, 827 (2006).

[75]M. Rambach, A. J. Bauer, and H. Ryssel, physica status solidi (b) **245**, 1315 (2008).

[76]H. Matsunami, Japanese Journal of Applied Physics **43**, 6835 (2004).

[77]J. V. Berens, *Carrier Mobility and Reliability of 4H-SiC Trench MOSFETs*, Ph.D. thesis, TU Wien (2021).

[78]H. Dixit, D. J. Lichtenwalner, A. Scholtze, J. H. Park, S. Rogers, S. Bubel, and S. H. Ryu, Materials Science Forum **1090**, 153 (2023).

[79]G. Izzo, G. Litrico, L. Calcagno, G. Foti, and F. La Via, Journal of Applied Physics **104**, 093711 (2008).

[80]F. La Via, G. Galvagno, F. Roccaforte, A. Ruggiero, and L. Calcagno, Applied Physics Letters **87**, 142105 (2005).

[81]S. Kagamihara, H. Matsuura, T. Hatakeyama, T. Watanabe, M. Kushibe, T. Shinohe, and K. Arai, Journal of Applied Physics **96**, 5601 (2004).

[82]H. Matsuura, M. Komeda, S. Kagamihara, H. Iwata, R. Ishihara, T. Hatakeyama, T. Watanabe, K. Kojima, T. Shinohe, and K. Arai, Journal of Applied Physics **96**, 2708 (2004).

[83]V. Uhnevionak, *Simulation and Modeling of Silicon-Carbide Devices*, Ph.D. thesis, Friedrich-Alexander-Universität (2015).

[84]K. Neimontas, T. Malinauskas, R. Aleksiejūnas, M. Sūdžius, K. Jarašiūnas, L. Storasta, J. P. Bergman, and E. Janzen, Semiconductor Science and Technology **21**, 952 (2006).

[85]T. T. Mnatsakanov, L. I. Pomortseva, and S. N. Yurkov, Semiconductors **35**, 394 (2001).

[86]D. Klaassen, Solid-State Electronics **35**, 953 (1992).

[87]S. K. Lee, *Processing and Characterization of Silicon Carbide (6H-SiC and 4H-SiC) Contacts for High Power and h...* (Mikroelektronik och informationsteknik, Kista, 2002).

[88]B. Chen, Y. Yang, X. Xie, N. Wang, Z. Ma, K. Song, and X. Zhang, Chinese Science Bulletin **57**, 4427 (2012).

[89]T. Kimoto and J. A. Cooper, *Fundamentals of Silicon Carbide Technology: Growth, Characterization, Devices, and Applications*, 1st ed. (Wiley, 2014).

[90]N. Lophitis, A. Arvanitopoulos, S. Perkins, and M. Antoniou, in *Disruptive Wide Bandgap Semiconductors, Related Technologies, and Their Applications*, edited by Y. K. Sharma (InTech, 2018).

[91]S. Banerjee, in *Advances in Terahertz Technology and Its Applications*, edited by S. Das, N. Anveshkumar, J. Dutta, and A. Biswas (Springer Singapore, Singapore, 2021) pp. 153–172.

[92]C. Canali, G. Majni, R. Minder, and G. Ottaviani, IEEE Transactions on Electron Devices **22**, 1045 (1975).

[93]S. Jin, K. Lee, W. Choi, C. Park, S. Yi, H. Fujii, J. Yoo, Y. Park, J. Jeong, and D. S. Kim, IEEE Transactions on Electron Devices , 1 (2024).

[94]A. E. Arvanitopoulos, M. Antoniou, S. Perkins, M. Jennings, M. B. Guadas, K. N. Gyftakis, and N. Lophitis, IEEE Transactions on Industry Applications **55**, 4080 (2019).

[95]C. Jacoboni, C. Canali, G. Ottaviani, and A. Alberigi Quaranta, Solid-State Electronics **20**, 77 (1977).

[96]J. Wang and B. W. Williams, Semiconductor Science and Technology **14**, 1088 (1999).

[97]S. M. Sze and K. K. Ng, *Physics of Semiconductor Devices*, 3rd ed. (Wiley-Interscience, Hoboken, N.J, 2007).

[98]K. Bertilsson, C. Harris, and H.-E. Nilsson, Solid-State Electronics **48**, 2103 (2004).

[99]S. Rakheja, L. Huang, S. Hau-Riege, S. E. Harrison, L. F. Voss, and A. M. Conway, IEEE Journal of the Electron Devices Society **8**, 1118 (2020).

[100]A. Akturk, N. Goldsman, S. Potbhare, and A. Lelis, Journal of Applied Physics **105**, 033703 (2009).

[101]E. Bellotti, *Advanced Modeling of Wide Band Gap Semiconductor Materials and Devices*, Ph.D. thesis, Georgia Institute of Technology (1999).

[102]E. Bellotti, H.-E. Nilsson, K. F. Brennan, P. P. Ruden, and R. Trew, Journal of Applied Physics **87**, 3864 (2000).

[103]K. Bertilsson, *Simulation and Optimization of SiC Field Effect Transistors*, Ph.D. thesis, Mikroelektronik och informationsteknik / KTH, Microelectronics and Information Technology, IMIT / KTH, Microelectronics and Information Technology, IMIT (2004).

[104]M. Hjelm, H.-E. Nilsson, A. Martinez, K. F. Brennan, and E. Bellotti, Journal of Applied Physics **93**, 1099 (2003).

[105]H.-E. Nilsson, E. Bellotti, K. Brennan, and M. Hjelm, Materials Science Forum **338–342**, 765 (2000).

[106]H.-E. Nilsson, U. Sannemo, and C. S. Petersson, Journal of Applied Physics **80**, 3365 (1996).

[107]B. Foutz, S. O'Leary, and M. Shur, in *High Power, Broadband, Linear, Solid State Amplifier* (Cornell University, 1998) p. 57.

[108]V. Polyakov and F. Schwierz, IEEE Transactions on Electron Devices **48**, 512 (2001).

[109]V. O. Turin, Solid-State Electronics **49**, 1678 (2005).

[110]J. Dorkel and Ph. Leturcq, Solid-State Electronics **24**, 821 (1981).

[111]S. C. Choo, IEEE Transactions on Electron Devices **19**, 954 (1972).

[112]S. Onoda, T. Ohshima, T. Hirao, K. Mishima, S. Hishiki, N. Iwamoto, and K. Kawano, IEEE Transactions on Nuclear Science **54**, 2706 (2007).

[113]S. Tripathi, C. Upadhyay, C. Nagaraj, A. Venkatesan, and K. Devan, Nuclear Instruments and Methods in Physics Research Section A: Accelerators, Spectrometers, Detectors and Associated Equipment **916**, 246 (2019).

[114]I.-R. Arvinte, *Investigation of Dopant Incorporation in Silicon Carbide Epilayers Grown by Chemical Vapor Deposition*, Ph.D. thesis, Universite Cote d'Azur (2017).

[115]G. Pensl, F. Schmid, F. Ciobanu, M. Laube, S. A. Reshanov, N. Schulze, K. Semmelroth, A. Schöner, G. Wagner, and H. Nagasawa, Materials Science Forum **433–436**, 365 (2003).

[116]S. Asada, T. Okuda, T. Kimoto, and J. Suda, Applied Physics Express **9**, 041301 (2016).

[117]S. Contreras, L. Konczewicz, P. Kwasnicki, R. Arvinte, H. Peyre, T. Chassagne, M. Zielinski, M. Kayambaki, S. Juillaguet, and K. Zekentes, Materials Science Forum **858**, 249 (2016).

[118]G. Rutsch, R. P. Devaty, W. J. Choyke, D. W. Langer, and L. B. Rowland, Journal of Applied Physics **84**, 2062 (1998).

[119]G. Pensl and W. Choyke, Physica B: Condensed Matter **185**, 264 (1993).

[120]M. Schadt, *Transporteigenschaften von Elektronen Und Löchern in Siliciumkarbid*, Ph.D. thesis, FriedrichAlexander-Universität (1997).

[121]A. Parisini and R. Nipoti, Journal of Applied Physics **114**, 243703 (2013).

[122]F. Schmid, M. Krieger, M. Laube, G. Pensl, and G. Wagner, in *Silicon Carbide*, edited by W. J. Choyke, H. Matsunami, and G. Pensl (Springer Berlin Heidelberg, Berlin, Heidelberg, 2004) pp. 517–536.

[123]D. K. Schroder, *Semiconductor Material and Device Characterization*, 1st ed. (Wiley, 2005).

[124]S. J. Bader, H. Lee, R. Chaudhuri, S. Huang, A. Hickman, A. Molnar, H. G. Xing, D. Jena, H. W. Then, N. Chowdhury, and T. Palacios, IEEE Transactions on Electron Devices **67**, 4010 (2020).

[125]M. Noguchi, T. Iwamatsu, H. Amishiro, H. Watanabe, K. Kita, and S. Yamakawa, in *2017 IEEE International Electron Devices Meeting (IEDM)* (IEEE, San Francisco, CA, USA, 2017) pp. 9.3.1–9.3.4.

[126]H. Tanaka and N. Mori, in *2024 International VLSI Symposium on Technology, Systems and Applications (VLSI TSA)* (IEEE, HsinChu, Taiwan, 2024) pp. 1–2.

[127]C. Weitzel, J. Palmour, C. Carter, and K. Nordquist, IEEE Electron Device Letters **15**, 406 (1994).

[128]H.-Y. Cha, Y. C. Choi, L. F. Eastman, M. G. Spencer, L. Ardaravicius, A. Matulionis, and O. Kiprijanovic, Journal of Electronic Materials **34**, 330 (2005).

[129]Y. Choi, H.-Y. Cha, L. Eastman, and M. Spencer, IEEE Transactions on Electron Devices **52**, 1940 (2005).

[130]Q. Zhang, A. Q. Huang, J. Wang, C. Jonas, R. Callanan, J. J. Sumakeris, S.-H. Ryu, M. Das, A. Agarwal, and J. Palmour, IEEE Transactions on Electron Devices **55**, 1912 (2008).

[131]H. A. Mantooth, K. Peng, E. Santi, and J. L. Hudgins, IEEE Transactions on Electron Devices **62**, 423 (2015).

[132]C. Persson and A. Ferreira Da Silva, in *Optoelectronic Devices: III Nitrides* (Elsevier, 2005) pp. 479–559.

[133]R. Trew, J.-B. Yan, and P. Mock, Proceedings of the IEEE **79**, 598 (1991).

[134]S. Murray and K. Roenker, Solid-State Electronics **46**, 1495 (2002).

[135]J. Vobecky, P. Hazdra, S. Popelka, and R. K. Sharma, IEEE Transactions on Electron Devices **62**, 1964 (2015).

[136]N. Wright, in *IEE Colloquium on New Developments in Power Semiconductor Devices*, Vol. 1996 (IEE, London, UK, 1996) pp. 6–6.

[137]N. G. Wright, D. Morrison, C. M. Johnson, and A. G. O'Neill, Materials Science Forum **264–268**, 917 (1998).

[138]K. Bertilsson, H.-E. Nilsson, M. Hjelm, C. Petersson, P. Käckell, and C. Persson, Solid-State Electronics **45**, 645 (2001).

[139]R. P. Joshi, Journal of Applied Physics **78**, 5518 (1995).

[140]C.-Y. Cheng and D. Vasileska, Journal of Applied Physics **127**, 155702 (2020).

[141]J. L. Vasconcelos, C. G. Rodrigues, and R. Luzzi, Materials Science and Engineering: B **249**, 114426 (2019).

[142]A. Martinez, U. Lindefelt, M. Hjelm, and H.-E. Nilsson, Journal of Applied Physics **91**, 1359 (2002).

[143]H. Iwata and K. M. Itoh, Materials Science Forum **338–342**, 729 (2000).

[144]T. Kinoshita, K. M. Itoh, J. Muto, M. Schadt, G. Pensl, and K. Takeda, Materials Science Forum **264–268**, 295 (1998).

[145]E. Belas, M. Betušiak, R. Grill, P. Praus, M. Brynza, J. Pipek, and P. Moravec, Journal of Alloys and Compounds **904**, 164078 (2022).

[146]L. Ardaravičius, A. Matulionis, O. Kiprijanovic, J. Liberis, H.-Y. Cha, L. F. Eastman, and

M. G. Spencer, Applied Physics Letters **86**, 022107 (2005).

[147]I. Khan and J. A. Cooper, Materials Science Forum **264–268**, 509 (1998).

[148]I. Khan and J. A. Cooper, Materials Science Forum **338–342**, 761 (2000).

[149]I. Khan and J. Cooper, IEEE Transactions on Electron Devices **47**, 269 (2000).

[150]V. Jaiswal and P. Vigneshwara Raja, IEEE Transactions on Nuclear Science , 1 (2024).

[151]S. Nakashima and H. Harima, physica status solidi (a) **162**, 39 (1997).

[152]M. K. Mainali, P. Dulal, B. Shrestha, E. Amonette, A. Shan, and N. J. Podraza, Surface Science Spectra **31**, 026003 (2024).

[153]N. T. Son, W. M. Chen, O. Kordina, A. O. Konstantinov, B. Monemar, E. Janzén, D. M. Hofman, D. Volm, M. Drechsler, and B. K. Meyer, Applied Physics Letters **66**, 1074 (1995).

[154]D. Werber, P. Borthen, and G. Wachutka, Materials Science Forum **556–557**, 905 (2007).

[155]D. L. Barrett and R. B. Campbell, Journal of Applied Physics **38**, 53 (1967).

[156]A. A. Burk, M. J. O'Loughlin, and S. Mani, Materials Science Forum **264–268**, 83 (1998).

[157]W. Choyke and G. Pensl, MRS Bulletin **22**, 25 (1997).

[158]S. Contreras, M. Zielinski, L. Konczewicz, C. Blanc, S. Juillaguet, R. Müller, U. Künecke, P. J. Wellmann, and J. Camassel, Materials Science Forum **527–529**, 633 (2006).

[159]H. Fujihara, J. Suda, and T. Kimoto, Japanese Journal of Applied Physics **56**, 070306 (2017).

[160]A. Galeckas, P. Grivickas, V. Grivickas, V. Bikbajevas, and J. Linnros, physica status solidi (a) **191**, 613 (2002).

[161]A. Itoh, H. Akita, T. Kimoto, and H. Matsunami, Applied Physics Letters **65**, 1400 (1994).

[162]L. Kasamakova-Kolaklieva, L. Storasta, I. G. Ivanov, B. Magnusson, S. Contreras, C. Consejo, J. Pernot, M. Zielinski, and E. Janzén, Materials Science Forum **457–460**, 677 (2004).

[163]T. Kimoto, S. Nakazawa, K. Hashimoto, and H. Matsunami, Applied Physics Letters **79**, 2761 (2001).

[164]M. Laube, F. Schmid, K. Semmelroth, G. Pensl, R. P. Devaty, W. J. Choyke, G. Wagner, and M. Maier, in *Silicon Carbide*, edited by W. J. Choyke, H. Matsunami, and G. Pensl (Springer Berlin Heidelberg, Berlin, Heidelberg, 2004) pp. 493–515.

[165]G. Lomakina, G. F. Kholuyanov, R. Verenehikova, E. Mokhov, and Y. A. Vodakov, Sov. Phys. Semiconductors **6**, 988 (1972).

[166]H. Matsunami and T. Kimoto, Materials Science and Engineering: R: Reports **20**, 125 (1997).

[167]H. Matsunami, Proceedings of the Japan Academy, Series B **96**, 235 (2020).

[168]R. Nipoti, R. Scaburri, A. Hallén, and A. Parisini, Journal of Materials Research **28**, 17 (2013).

[169]G. Pensl, F. Ciobanu, T. Frank, M. Krieger, S. Reshanov, F. Schmid, and M. Weidner, International Journal of High Speed Electronics and Systems **15**, 705 (2005).

[170]M. Schadt, G. Pensl, R. P. Devaty, W. J. Choyke, R. Stein, and D. Stephani, Applied Physics Letters **65**, 3120 (1994).

[171]A. Schöner, *Elektrische Charakterisierung von Flachen Und Tiefen Störstellen in 4H-, 6H- Und 15R-Siliziumkarbid*, Ph.D. thesis, FriedrichAlexander-Universität (1994).

[172]A. Schöner, S. Karlsson, T. Schmitt, N. Nordell, M. Linnarsson, and K. Rottner, Materials Science and Engineering: B **61–62**, 389 (1999).

[173]R. Siergiej, R. Clarke, S. Sriram, A. Agarwal, R. Bojko, A. Morse, V. Balakrishna, M. MacMillan, A. Burk, Jr, and C. Brandt, Materials Science and Engineering: B **61–62**, 9 (1999).

[174]P. Terziyska, C. Blanc, J. Pernot, H. Peyre, S. Contreras, G. Bastide, J. L. Robert, J. Camassel, E. Morvan, C. Dua, and C. C. Brylinski, physica status solidi (a) **195**, 243 (2003).

[175]G. Rutsch, R. P. Devaty, W. J. Choyke, D. Langer, L. Rowland, E. Niemann, and F. Wischmeyer, Materials Science Forum **338–342**, 733 (2000).

[176]H. Habib, N. G. Wright, and A. B. Horsfall, Advanced Materials Research **413**, 229 (2011).

[177]M. Willander, M. Friesel, Q.-u. Wahab, and B. Straumal, Journal of Materials Science: Materials in Electronics **17**, 1 (2006).

[178]A. Elasser, M. Kheraluwala, M. Ghezzo, R. Steigerwald, N. Evers, J. Kretchmer, and T. Chow, IEEE Transactions on Industry Applications **39**, 915 (2003).

[179]R. Trew, Proceedings of the IEEE **90**, 1032 (2002).

[180]A. Elasser, M. Ghezzo, N. Krishnamurthy, J. Kretchmer, A. Clock, D. Brown, and T. Chow, Solid-State Electronics **44**, 317 (2000).

[181]R. J. Trew, physica status solidi (a) **162**, 409 (1997).

[182]J. I. Pankove, ed., *Electroluminescence*, softcover reprint of the original 1st ed. 1977 ed. (Springer Berlin, Berlin, 2014).

[183]V. R. Manikam and Kuan Yew Cheong, IEEE Transactions on Components, Packaging and Manufacturing Technology **1**, 457 (2011).

[184]J. Hudgins, G. Simin, E. Santi, and M. Khan, IEEE Transactions on Power Electronics **18**, 907 (2003).

[185]N. Zhang, *High Voltage GaN HEMTs with Low On-Resistance for Switching Applications*, Ph.D. thesis, UNIVERSITY of CALIFORNIA, Santa Barbara (2002).

[186]R. Kemerley, H. Wallace, and M. Yoder, Proceedings of the IEEE **90**, 1059 (2002).

[187]G. Pacchioni, L. Skuja, and D. L. Griscom, eds., *Defects in SiO2 and Related Dielectrics: Science and Technology* (Springer Netherlands, Dordrecht, 2000).

[188]V. V. Afanas'ev, A. Stesmans, M. Bassler, G. Pensl, and M. J. Schulz, Applied Physics Letters **76**, 336 (2000).

[189]WJ. Choyke and L. Patrick, in *In: Silicon Carbide-1973; Proceedings of the Third International Conference* (1974) pp. 261–283.

[190]M. Su, *Power Devices and Integrated Circuits Based on 4H-SiC Lateral JFETs*, Ph.D. thesis, New Brunswick Rutgers, New Jersey (2010).

[191]P. Masri, Surface Science Reports **48**, 1 (2002).

[192]A. Itoh, T. K. Tsunenobu Kimoto, and H. M. Hiroyuki Matsunami, Japanese Journal of Applied Physics **35**, 4373 (1996).

[193]A. Itoh, T. Kimoto, and H. Matsunami, IEEE Electron Device Letters **16**, 280 (1995).

[194]T. Kimoto, A. Itoh, and H. Matsunami, physica status solidi (b) **202**, 247 (1997).

[195]V. Soler, *Design and Process Developments towards an Optimal 6.5 kV SiC Power MOSFET*, Ph.D. thesis, Universitat Politecnica de Catalunya (2019).

[196]M. De Napoli, Frontiers in Physics **10**, 898833 (2022).

[197]A. Hassan, Y. Savaria, and M. Sawan, IEEE Access **6**, 78790 (2018).

[198]S. Rybalka, E.Yu. Krayushkina, A. Demidov, O. Shishkina, and B. Surin, International Journal of Physical Research **5**, 11 (2017).

[199]H. Choi, "Overview of Silicon Carbide Power Devices," (2016).

[200]P. G. Neudeck, in *Extreme Environment Electronics* (CRC Press, Taylor & Francis Group, 2013) pp. 225–232.

[201]H. A. Mantooth, in *Extreme Environment Electronics* (CRC Press, Taylor & Francis Group, 2013) pp. 243–252.

[202]F. Nava, G. Bertuccio, A. Cavallini, and E. Vittone, Measurement Science and Technology **19**, 102001 (2008).

[203]J. H. Zhao, K. Sheng, and R. C. Lebron-Velilla, "SILICON CARBIDE SCHOTTKY BARRIER DIODE," in *Sic Materials and Devices*, Vol. 40 (WORLD SCIENTIFIC, 2006) pp. 117–162.

[204]M. E. Levinshtein, T. T. Mnatsakanov, P. A. Ivanov, R. Singh, J. W. Palmour, and S. N. Yurkov, Solid-State Electronics **48**, 807 (2004).

[205]B. Ng, J. David, R. Tozer, G. Rees, Feng Yan, Jian H. Zhao, and M. Weiner, IEEE Transactions

on Electron Devices **50**, 1724 (2003).

[206] A. A. Lebedev, Semiconductors **33**, 107 (1999).

[207] A. Burk, M. O'Loughlin, R. Siergiej, A. Agarwal, S. Sriram, R. Clarke, M. MacMillan, V. Balakrishna, and C. Brandt, Solid-State Electronics **43**, 1459 (1999).

[208] A. Agarwal, S. Seshadri, J. Casady, S. Mani, M. MacMillan, N. Saks, A. Burk, G. Augustine, V. Balakrishna, P. Sanger, C. Brandt, and R. Rodrigues, Diamond and Related Materials **8**, 295 (1999).

[209] V. Chelnokov and A. Syrkin, Materials Science and Engineering: B **46**, 248 (1997).

[210] A. Agarwal, G. Augustine, V. Balakrishna, C. Brandt, A. Burk, Li-Shu Chen, R. Clarke, P. Esker, H. Hobgood, R. Hopkins, A. Morse, L. Rowland, S. Seshadri, R. Siergiej, T. Smith, and S. Sriram, in *International Electron Devices Meeting. Technical Digest* (IEEE, San Francisco, CA, USA, 1996) pp. 225–230.

[211] P. G. Neudeck, Journal of Electronic Materials **24**, 283 (1995).

[212] N. S. Saks, S. S. Mani, and A. K. Agarwal, Applied Physics Letters **76**, 2250 (2000).

[213] R. Choudhary, M. Mehta, R. Singh Shekhawat, S. Singh, and D. Singh, Materials Today: Proceedings **46**, 5889 (2021).

[214] P. Luo and S. N. E. Madathil, IEEE Transactions on Electron Devices **67**, 5621 (2020).

[215] M. Cabello, V. Soler, G. Rius, J. Montserrat, J. Rebollo, and P. Godignon, Materials Science in Semiconductor Processing **78**, 22 (2018).

[216] S. Fujita, Japanese Journal of Applied Physics **54**, 030101 (2015).

[217] N. Kaminski and O. Hilt, IET Circuits, Devices & Systems **8**, 227 (2014).

[218] J. A. Pellish and L. M. Cohn, in *Extreme Environment Electronics* (CRC Press, Taylor & Francis Group, 2013) pp. 49–58.

[219] M. Ostling, R. Ghandi, and C.-M. Zetterling, in *2011 IEEE 23rd International Symposium on Power Semiconductor Devices and ICs* (IEEE, San Diego, CA, USA, 2011) pp. 10–15.

[220] M. Östling, Science China Information Sciences **54**, 1087 (2011).

[221] K. G. Menon, A. Nakajima, L. Ngwendson, and E. M. Sankara Narayanan, IEEE Electron Device Letters **32**, 1272 (2011).

[222] C. Buttay, D. Planson, B. Allard, D. Bergogne, P. Bevilacqua, C. Joubert, M. Lazar, C. Martin, H. Morel, D. Tournier, and C. Raynaud, Materials Science and Engineering: B **176**, 283 (2011).

[223] N. Kaminski, 2009 13th European Conference on Power Electronics and Applications **8** (2009).

[224] J. Millán, IET Circuits, Devices & Systems **1**, 372 (2007).

[225]D. T. Morisette, *Development of Robust Power Schottky Barrier Diodes in Silicon Carbide*, Ph.D. thesis, Purdue University (2001).

[226]X. Guo, Q. Xun, Z. Li, and S. Du, Micromachines **10**, 406 (2019).

[227]J. Y. Tsao, S. Chowdhury, M. A. Hollis, D. Jena, N. M. Johnson, K. A. Jones, R. J. Kaplar, S. Rajan, C. G. Van De Walle, E. Bellotti, C. L. Chua, R. Collazo, M. E. Coltrin, J. A. Cooper, K. R. Evans, S. Graham, T. A. Grotjohn, E. R. Heller, M. Higashiwaki, M. S. Islam, P. W. Juodawlkis, M. A. Khan, A. D. Koehler, J. H. Leach, U. K. Mishra, R. J. Nemanich, R. C. N. Pilawa-Podgurski, J. B. Shealy, Z. Sitar, M. J. Tadjer, A. F. Witulski, M. Wraback, and J. A. Simmons, Advanced Electronic Materials **4**, 1600501 (2018).

[228]S. J. Pearton, X. Xia, F. Ren, M. A. J. Rasel, S. Stepanoff, N. Al-Mamun, A. Haque, and D. E. Wolfe, Journal of Vacuum Science & Technology B **41**, 030802 (2023).

[229]S. J. Pearton, J. Yang, P. H. Cary, F. Ren, J. Kim, M. J. Tadjer, and M. A. Mastro, Applied Physics Reviews **5**, 011301 (2018).

[230]J. Lutz, U. Scheuermann, H. Schlangenotto, and R. De Doncker, "Power Semiconductor Devices—Key Components for Efficient Electrical Energy Conversion Systems," in *Semiconductor Power Devices* (Springer International Publishing, Cham, 2018) pp. 1–20.

[231]M. Higashiwaki, K. Sasaki, A. Kuramata, T. Masui, and S. Yamakoshi, physica status solidi (a) **211**, 21 (2014).

[232]S. Sandeep and R. Komaragiri, in *India International Conference on Power Electronics 2010 (IICPE2010)* (IEEE, New Delhi, India, 2011) pp. 1–5.

[233]R. Gerhardt, ed., *Properties and Applications of Silicon Carbide* (IntechOpen, 2011).

[234]B. Ozpineci, "Comparison of Wide-Bandgap Semiconductors for Power Electronics Applications," Tech. Rep. ORNL/TM-2003/257, 885849 (Oak Ridge National Laboratory, 2004).

[235]A. Powell and L. Rowland, Proceedings of the IEEE **90**, 942 (2002).

[236]M. Werner and W. Fahrner, IEEE Transactions on Industrial Electronics **48**, 249 (2001).

[237]A. O. Evwaraye, S. R. Smith, and W. C. Mitchel, Journal of Applied Physics **79**, 7726 (1996).

[238]J. Casady and R. Johnson, Solid-State Electronics **39**, 1409 (1996).

[239]M. Yoder, IEEE Transactions on Electron Devices **43**, 1633 (1996).

[240]G. Lomakina, in *In: Silicon Carbide-1973; Proceedings of the Third International Conference* (1974) pp. 520–526.

[241]T. P. Chow, I. Omura, M. Higashiwaki, H. Kawarada, and V. Pala, IEEE Transactions on Electron Devices **64**, 856 (2017).

[242]G. Dhanaraj, K. Byrappa, V. Prasad, and M. Dudley, eds., *Springer Handbook of Crystal Growth* (Springer Berlin Heidelberg, Berlin, Heidelberg, 2010).

[243]P. B. Klein, physica status solidi (a) **206**, 2257 (2009).

[244]M. W. Cole and P. Joshi, in *Silicon Carbide*, edited by Z. C. Feng and J. H. Zhao (Springer Berlin Heidelberg, Berlin, Heidelberg, 2004) pp. 517–536.

[245]T. P. Chow, N. Ramungul, J. Fedison, and Y. Tang, in *Silicon Carbide*, edited by W. J. Choyke, H. Matsunami, and G. Pensl (Springer Berlin Heidelberg, Berlin, Heidelberg, 2004) pp. 737–767.

[246]A. Elasser and T. Chow, Proceedings of the IEEE **90**, 969 (2002).

[247]V. Dmitriev, T. P. Chow, S. P. DenBaars, M. S. Shur, and M. G. Spencer, "High-Temperature Electronics in Europe:," Tech. Rep. (Defense Technical Information Center, Fort Belvoir, VA, 2000).

[248]T. Chow, V. Khemka, J. Fedison, N. Ramungul, K. Matocha, Y. Tang, and R. Gutmann, Solid-State Electronics **44**, 277 (2000).

[249]T. P. Chow, Materials Science Forum **338–342**, 1155 (2000).

[250]T. P. Chow, N. Ramungul, and M. Ghezzo, MRS Proceedings **483**, 89 (1997).

[251]T. P. Chow and M. Ghezzo, MRS Proceedings **423**, 9 (1996).

[252]D. Mukherjee and M. Neto, *Recent Advances in SiC/Diamond Composite Devices* (IOP Publishing, 2023).

[253]M. B. Wijesundara and R. Azevedo, *Silicon Carbide Microsystems for Harsh Environments*, MEMS Reference Shelf, Vol. 22 (Springer New York, New York, NY, 2011).

[254]X. Zhu, *ALTERNATIVE GROWTH AND INTERFACE PASSIVATION TECHNIQUES FOR SiO2 ON 4H-SiC*, Ph.D. thesis, Auburn University (2008).

[255]P. G. Neudeck (CRC Press, 2006).

[256]P. Neudeck, in *Encyclopedia of Materials: Science and Technology* (Elsevier, 2001) pp. 8508–8519.

[257]C. Weitzel, Materials Science Forum **264–268**, 907 (1998).

[258]S. Sriram, R. R. Siergiej, R. C. Clarke, A. K. Agarwal, and C. D. Brandt, physica status solidi (a) **162**, 441 (1997).

[259]C. Weitzel, J. Palmour, C. Carter, K. Moore, K. Nordquist, S. Allen, C. Thero, and M. Bhatnagar, IEEE Transactions on Electron Devices **43**, 1732 (1996).

[260]C.-M. Zetterling, ed., *Process Technology for Silicon Carbide Devices*, EMIS Processing Series

No. 2 (Institution of Electrical Engineers, London, 2002).

[261]J. Palmour, R. Singh, R. Glass, O. Kordina, and C. Carter, in *Proceedings of 9th International Symposium on Power Semiconductor Devices and IC's* (IEEE, Weimar, Germany, 1997) pp. 25–32.

[262]I. Capan, Electronics **11**, 532 (2022).

[263]G. Rescher, *Behavior of SiC-MOSFETs under Temperature and Voltage Stress*, Ph.D. thesis, TU Wien (2018).

[264]T. Kimoto, Japanese Journal of Applied Physics **54**, 040103 (2015).

[265]C. Langpoklakpam, A.-C. Liu, K.-H. Chu, L.-H. Hsu, W.-C. Lee, S.-C. Chen, C.-W. Sun, M.-H. Shih, K.-Y. Lee, and H.-C. Kuo, Crystals **12**, 245 (2022).

[266]G. Liu, B. R. Tuttle, and S. Dhar, Applied Physics Reviews **2**, 021307 (2015).

[267]R. Raghunathan and B. Baliga, IEEE Electron Device Letters **19**, 71 (1998).

[268]F. C. Beyer, *Deep Levels in SiC*, Ph.D. thesis, Linköping University (2011).

[269]M. E. Levinshteĭn, S. L. Rumyantsev, and M. Shur, eds., *Properties of Advanced Semiconductor Materials: GaN, AlN, InN, BN, SiC, SiGe* (Wiley, New York, 2001).

[270]P. Bhatnagar, A. B. Horsfall, N. G. Wright, C. M. Johnson, K. V. Vassilevski, and A. G. O'Neill, Solid-State Electronics **49**, 453 (2005).

[271]S. Bellone and L. Di Benedetto, IEEE Transactions on Power Electronics **29**, 2174 (2014).

[272]L. Di Benedetto, G. D. Licciardo, R. Nipoti, and S. Bellone, IEEE Electron Device Letters **35**, 244 (2014).

[273]I. Institute, "Silicon Carbide," http://www.ioffe.ru/SVA/NSM/Semicond/SiC/index.html (2023).

[274]G. Lomakina and Y. A. Vodakov, Sov. Phys. Solid State **15**, 83 (1973).

[275]D. Johannesson, M. Nawaz, and H. P. Nee, Materials Science Forum **963**, 670 (2019).

[276]Q. Chen, L. Yang, S. Wang, Y. Zhang, Y. Dai, and Y. Hao, Applied Physics A **118**, 1219 (2015).

[277]R. Mickevičius and J. H. Zhao, Materials Science Forum **264–268**, 291 (1998).

[278]M. Ruff, H. Mitlehner, and R. Helbig, IEEE Transactions on Electron Devices **41**, 1040 (1994).

[279]M. Roschke, F. Schwierz, G. Paasch, and D. Schipanski, Materials Science Forum **264–268**, 965 (1998).

[280]S. Balachandran, T. P. Chow, and A. K. Agarwal, Materials Science Forum **483–485**, 909 (2005).

[281]S. Rao, E. D. Mallemace, and F. G. Della Corte, Electronics **11**, 1839 (2022).

[282]G. L. Harris and Inspec, eds., *Properties of Silicon Carbide*, EMIS Datareviews Series No. 13 (INSPEC, the Inst. of Electrical Engineers, London, 1995).

[283]C. Carter, Jr., V. Tsvetkov, R. Glass, D. Henshall, M. Brady, St.G. Müller, O. Kordina, K. Irvine, J. Edmond, H.-S. Kong, R. Singh, S. Allen, and J. Palmour, Materials Science and Engineering: B **61–62**, 1 (1999).

[284]S. Nakashima and H. Harima, SILICON CARBIDE AND RELATED MATERIALS 1995 **142**, 269 (1996).

[285]M. Nawaz, Microelectronics Journal **41**, 801 (2010).

[286]M. Usman and M. Nawaz, Solid-State Electronics **92**, 5 (2014).

[287]F. Nallet, A. Senes, D. Planson, M. Locatelli, J. Chante, and J. Taboy, in *Proceedings IPEMC 2000. Third International Power Electronics and Motion Control Conference (IEEE Cat. No.00EX435)*, Vol. 1 (Int. Acad. Publishers, Beijing, China, 2000) pp. 396–401.

[288]T. Tamaki, G. G. Walden, Y. Sui, and J. A. Cooper, IEEE Transactions on Electron Devices **55**, 1920 (2008).

[289]H. Liu, J. Wang, S. Liang, H. Yu, and W. Deng, Semiconductor Science and Technology **36**, 025009 (2021).

[290]T. R. McNutt, in *Extreme Environment Electronics* (CRC Press, Taylor & Francis Group, 2013) pp. 409–416.

[291]P. B. Shah and K. A. Jones, Journal of Applied Physics **84**, 4625 (1998).

[292]J. Wang and B. W. Williams, Semiconductor Science and Technology **13**, 806 (1998).

[293]J. Zhao, X. Li, K. Tone, P. Alexandrov, M. Pan, and M. Weiner, Solid-State Electronics **47**, 377 (2003).

[294]T. Yang, Y. Tan, C. Wang, X. Zhang, and X. Shi, "Simulation of the 4H-SiC Low Gain Avalanche Diode," (2022), arXiv:2206.10191 [physics].

[295]S. I. Maximenko, AIP Advances **13**, 105021 (2023).

[296]Y.-R. zhang, b. zhang, Z.-J. Li, X.-C. Deng, and X.-L. liu, Chinese Physics B **18**, 3995 (2009).

[297]M. Khalid, S. Riaz, and S. Naseem, Communications in Theoretical Physics **58**, 577 (2012).

[298]D. Johannesson and M. Nawaz, IEEE Transactions on Power Electronics **31**, 4517 (2016).

[299]V. Tilak, K. Matocha, and G. Dunne, IEEE Transactions on Electron Devices **54**, 2823 (2007).

[300]S. Bellone, F. G. Della Corte, L. F. Albanese, and F. Pezzimenti, IEEE Transactions on Power Electronics **26**, 2835 (2011).

[301]F. Pezzimenti, IEEE Transactions on Electron Devices **60**, 1404 (2013).

[302]M. L. Megherbi, L. Dehimi, W. terghini, F. Pezzimenti, and F. G. Della Corte, Courrier du Savoir **19**, 71 (2015).

[303]Y. Zhou, Y. Li, and B. Wang, in *2016 IEEE 4th Workshop on Wide Bandgap Power Devices and Applications (WiPDA)* (IEEE, Fayetteville, AR, 2016) pp. 1–7.

[304]K. Zeghdar, L. Dehimi, F. Pezzimenti, S. Rao, and F. G. Della Corte, Japanese Journal of Applied Physics **58**, 014002 (2019).

[305]K. Zeghdar, L. Dehimi, F. Pezzimenti, M. L. Megherbi, and F. G. Della Corte, Journal of Electronic Materials **49**, 1322 (2020).

[306]R. Nipoti, A. Parisini, G. Sozzi, M. Puzzanghera, A. Parisini, and A. Carnera, ECS Journal of Solid State Science and Technology **5**, P621 (2016).

[307]D. Brosselard, Pierre ; Planson, *Conception, Réalisation et Caractérisation d'interrupteurs (Thyristors et JFETs) Haute Tension (5kV) En Carbure de Silicium*, Ph.D. thesis (2004).

[308]T. Hatakeyama, T. Watanabe, T. Shinohe, K. Kojima, K. Arai, and N. Sano, Applied Physics Letters **85**, 1380 (2004).

[309]V. I. Sankin and A. A. Lepneva, Materials Science Forum **338–342**, 769 (2000).

[310]K. Vassilevski, K. Zekentes, A. Zorenko, and L. Romanov, IEEE Electron Device Letters **21**, 485 (2000).

[311]W. V. Muench and E. Pettenpaul, Journal of Applied Physics **48**, 4823 (1977).

[312]A. A. Lebedev, *Radiation Effects in Silicon Carbide*, Materials Research Foundations No. volume 6 (2017) (Materials Research Forum LLC, Millersville, PA, USA, 2017).

[313]S. Reshanov, *Device-relevant defect centers and minority carrier lifetime in 3C-, 4H- and 6H-SiC*, Ph.D. thesis, Friedrich-Alexander-Universität, Erlangen-Nürnberg (2005).

[314]R. Han, X. Xu, X. Hu, N. Yu, J. Wang, Y. Tian, and W. Huang, Optical Materials **23**, 415 (2003).

[315]S. Doğan, F. Yun, C. Roberts, J. Parish, D. Huang, R. E. Myers, M. Smith, S. E. Saddow, B. Ganguly, and H. Morkoç, MRS Proceedings **764**, C7.2 (2003).

[316]M. Bhatnagar and B. Baliga, IEEE Transactions on Electron Devices **40**, 645 (1993).

[317]J. A. Powell and L. G. Matus, in *Amorphous and Crystalline Silicon Carbide II*, Vol. 43, edited by H. K. V. Lotsch, M. M. Rahman, C. Y.-W. Yang, and G. L. Harris (Springer Berlin Heidelberg, Berlin, Heidelberg, 1989) pp. 14–19.

[318]N. Fletcher, Proceedings of the IRE **45**, 862 (1957).